

Self-Configurable Mesh-Networks for Scalable Distributed Submodular Bandit Optimization

Zirui Xu, Vasileios Tzoumas[†]

Abstract—We study how to scale distributed bandit submodular coordination under realistic communication constraints in bandwidth, data rate, and connectivity. We are motivated by multi-agent tasks of active situational awareness in unknown, partially-observable, and resource-limited environments, where the agents must coordinate through agent-to-agent communication. Our approach enables scalability by (i) limiting information relays to only one-hop communication and (ii) keeping inter-agent messages small, having each agent transmit only its own action information. Despite these information-access restrictions, our approach enables near-optimal action coordination by optimizing the agents’ communication neighborhoods over time, through distributed online bandit optimization, subject to the agents’ bandwidth constraints. Particularly, our approach enjoys an anytime suboptimality bound that is also strictly positive for arbitrary network topologies, even disconnected. To prove the bound, we define the *Value of Coordination* (VoC), an information-theoretic metric that quantifies for each agent the benefit of information access to its neighbors. We validate in simulations the scalability and near-optimality of our approach: it is observed to converge faster, outperform benchmarks for bandit submodular coordination, and can even outperform benchmarks that are privileged with a priori knowledge of the environment.

I. INTRODUCTION

In the future, large-scale teams of distributed agents will be executing sensing-driven tasks such as target tracking [1], environmental mapping [2], and area monitoring [3]. These collaborative tasks require the distributed agents to share their local observations—expand information access—to improve coordination performance. However, expanding information access is challenging due to the limited communication, computing, and sensing capabilities onboard each agent, and the above tasks often operate in unknown, unstructured, and dynamic environments. In more detail, several challenges to scalability and optimality appear:

(a) *Limited communication bandwidth*: Each agent can communicate with only a limited number of peers at a time, rather than with all physically reachable ones [4], [5].

(b) *Finite data rate*: Communication occurs via onboard radio modules with restricted data rates, ranging from as low as 0.25 Mbps (e.g., Digi XBee 3 Zigbee 3 [6]) to around 100 Mbps (e.g., Silvus Tech SL5200 [7]), far below the 0.8–1.5 Gbps commonly available in everyday Wi-Fi 6 systems [8].

(c) *Unguaranteed network connectivity*: Agents may receive information only from those within a fixed communication range or line of sight, meaning the communication graph is not guaranteed to remain connected [9].

(d) *Unstructured environment*: The environment may be unknown a priori and partially observable. Thus, the informational value of each observation becomes known only once the observation is made. This optimization setting corresponds to the *bandit* feedback model [10].

These challenges motivate distributed optimization problems in bandit settings [10] for *large-scale* tasks in robotics, control, and machine learning. Such joint optimization problems often take the form of

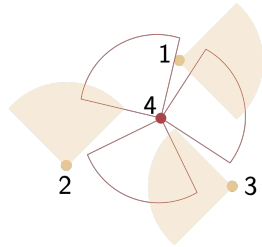
$$\max_{a_{i,t} \in \mathcal{V}_i, \forall i \in \mathcal{N}, \forall t \in [T]} \sum_{t=1}^T f(\{a_{i,t}\}_{i \in \mathcal{N}}), \quad (1)$$

where T is the operation time-horizon, and at each time step $t \in [T]$, the agents \mathcal{N} need to each select an action $a_{i,t}$ from its available action set \mathcal{V}_i to collaboratively maximize the unknown a priori objective function $f: 2^{\prod_{i \in \mathcal{N}} \mathcal{V}_i} \mapsto \mathbb{R}$ that captures the task utility [2], [3], [11]–[21]. In information-gathering tasks, f is often *submodular* [22]: submodularity is a diminishing returns property, and it emanates due to the possible information overlap among the information gathered by the agents [11]. For example, in target monitoring with multiple cameras at fixed locations, \mathcal{N} is the set of cameras, \mathcal{V}_i is the available directions the camera can choose, and f is the number of targets covered by the cameras’ collective field of view (FOV). The cameras have no prior knowledge of target locations and can observe them only when they fall within the cameras’ collective FOV; targets that remain uncovered are therefore unknown to the cameras. As a result, the cameras can accurately evaluate only the utility of the FOVs they actually choose, which corresponds to the bandit feedback setting [10].

The optimization problem in eq. (1) is NP-hard even in known environments [23]. Polynomial-time algorithms with provable approximation guarantees exist. A classical example is the Sequential Greedy (SG) algorithm [22], which achieves a 1/2-approximation ratio. Since many multi-agent tasks, such as target tracking, collaborative mapping, and area monitoring, can be formulated as submodular coordination problems, SG and its variants have been widely adopted across the controls, machine learning, and robotics communities [2], [3], [11]–[14], [16], [17], [19]–[21], [24]–[26]. In unknown environments instead, online variants of SG are proposed [1], [27]–[33], providing guaranteed suboptimality over the horizon T . Continuous-domain optimization techniques have also been leveraged in the bandit setting by first using the multilinear extension [34], to lift the discrete submodular function f to the continuous domain, then applying gradient/consensus-based techniques, and finally rounding back to the discrete domain to obtain a near-optimal solution [20], [32], [35]–[37].

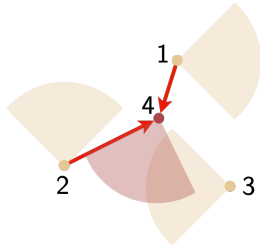
[†]Department of Aerospace Engineering, University of Michigan, Ann Arbor, MI 48109 USA; {ziruiXu,vtzoumas}@umich.edu

Camera 4 needs to select its FOV from three options w/ comm. bandwidth = 2



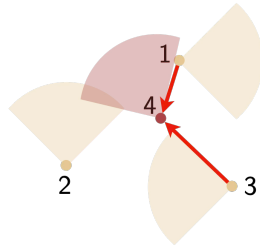
(a) Area monitoring setup

Listen to 1 & 2; no info about 3



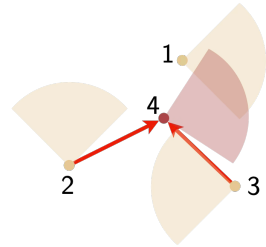
(b) Comm. neighborhood design 1

Listen to 1 & 3; no info about 2



(c) Comm. neighborhood design 2 (Best)

Listen to 2 & 3; no info about 1



(d) Comm. neighborhood design 3

Fig. 1: **Information Access Matters: A Multi-Camera Area Monitoring Example.** Consider a multi-camera area monitoring task where four cameras must coordinate their fields of view (FOVs) via distributed communication to maximize total coverage. As shown in (a), suppose that cameras 1–3 have already fixed their FOVs (soft orange), and camera 4 must select its FOV from three predefined options (dark red). While the optimal choice for camera 4 depends on the FOVs of all other three, its communication bandwidth allows it to receive information from at most two of them at any current time. The three possible communication neighborhood configurations and the corresponding FOV selections are demonstrated in (b)–(d), among which the design in (c) yields the highest coverage and therefore the optimal FOV decision. This example illustrates that intelligent information access—enabled by active neighborhood design (possibly over multiple time steps)—can optimize action coordination performance in distributed settings with limited communication resources.

However, the algorithms above cannot scale as the network grows when challenges (a)–(d) exist simultaneously. In particular, current distributed approaches, based on either sequential communication in the discrete domain [1], [2], [33] or repeated consensus iterations in the continuous domain [20], [24], [27]–[32], [35]–[37], assume instantaneous agent-to-agent communication, *i.e.*, infinite data rates. But if accounting for the limited data rates of onboard radio modules, per challenge (b), decision times of these methods can scale cubically in network size or even more [21, Table 1]. This is due to:

- *Message size:* The size of communication messages can scale proportionally with the number of agents.
- *Information relay:* Distributed agents use multi-hop relays to expand information access.

In sum, under challenges (a)–(d), where instantaneous communication is infeasible and the environment is unknown, achieving both scalability and optimality requires *restricting information access intelligently*, via limiting message size and/or information relay, to balance the trade-off between decision time and decision optimality. Methods in [38], [39] leverage communication quantization to shorten messages and evaluate its effect on optimality. The framework in [40] reduces communication overhead by exploiting the sparsity of the underlying information dependence among agents and omitting information sharing between agents with low dependence accordingly. It also establishes the necessary conditions for convergence. However, the approaches in [38]–[40] focus on convex optimization. In discrete submodular optimization, the focus of this paper, current works [14]–[16] only perform f -agnostic communication restriction, *i.e.*, the topology designed will remain the same, independently of the f specified by the application. In more detail, [14]–[16] study a variant of SG with restricted information relay where each agent i receives information from only a subset rather than all of $\{1, \dots, i-1\}$ as in the classical SG.¹ These works derive suboptimality bounds that scale inversely with the indepen-

¹In discrete submodular optimization, agents perform sequential communication, where message complexity depends on the network topology. For example, in a line network, a message from agent $i-1$ to i may aggregate information from all preceding agents $\{1, \dots, i-1\}$, whereas in a complete network it contains only agent $i-1$'s data, with other information transmitted through separate links.

dence number of the resulting information-sharing topology,² and further propose a centralized information-sharing topology design method based on these bounds [16]. The recent algorithm in [21] restricts information access within one-hop neighbors, thus prohibiting relays and having each agent-to-agent message to contain information only about the agent that transmits it. It also enables partially parallelized action selection to reduce communication latency. Although [21] characterizes f -specific coordination performance, the bound is intractable to optimize even in hindsight, and therefore cannot support intelligent information access restriction.

Contributions. We provide a distributed multi-agent decision-making framework that enables both scalable and near-optimal action coordination in unknown environments under realistic communication constraints in bandwidth, data rate, and connectivity. Our approach enables scalability by (i) limiting information relays to only one-hop communication and (ii) keeping inter-agent messages small, having each agent transmit only its own action information. Despite these information-access restrictions, our approach improves the near-optimality bound of action coordination by optimizing the agents' communication neighborhoods over time, through distributed online bandit optimization (subject to the agents' bandwidth constraints)—the necessity for such information access optimization is demonstrated in Fig. 1.

To our knowledge, this is the first rigorous approach that enables multi-agent networks to scale near-optimal coordination by actively optimizing the restricted information access through active communication topology self-configuration. The approach is fully distributed: each agent jointly selects its action and designs its local communication neighborhood subject to its coordination neighborhood and bandwidth constraints. The algorithm has the following properties:

a) Scalability: ANACONDA enjoys improved scalability under communication constraints by having a convergence time of $O(|\mathcal{N}|^2)$ in sparse networks, accounting for information relay in multi-hop communication (Section V). This is faster than existing methods even though they only consider known environments [21, Table I]. In practice, the algorithm

²This information-sharing topology is the Directed Acyclic Graph (DAG) derived from the communication network.

can converge even faster, *e.g.*, only sublinearly in $|\mathcal{N}|$ in the area monitoring simulations (Section VII-D).

b) Anytime Self-Configuration with Arbitrary Topologies: ANACONDA enables each agent to adapt its communication neighborhood online according to the given f , resulting in coordination over a directed, time-varying, and potentially disconnected network. The fully distributed self-configuration mechanism further allows agents to join or leave the system without disrupting the co-optimization process. Our prior work [21], instead, does not optimize the network; [16] performs network design centrally without leveraging f ; and [1]–[3], [17], [19], [20], [24], [25], [33] require connected networks.

c) Approximation Performance: ANACONDA enjoys anytime, strictly positive, f -specific suboptimality bounds against an optimal solution of eq. (1) (Section IV). The bounds capture the benefit of information access for each agent and thus remain valid under arbitrarily optimized communication topologies, regardless of global connectivity. In particular, Theorem 1, along with our numerical evaluations, validates that coordination performance improves through network optimization, and Theorems 2 and 3 ensure that ANACONDA achieves strictly positive performance guarantees at all times. The bounds in [14]–[16] are instead f -agnostic; the bound in our prior work [21] does not support network optimization; and [1]–[3], [17], [19], [20], [24], [25], [33] provide suboptimality guarantees only under connected network assumptions.

Numerical evaluations. We validate ANACONDA through simulations of multi-camera area monitoring. The results first show that the proposed information-driven neighbor selection strategy outperforms typical baselines (nearest and random neighbors) in robotics and controls [21], [41], [42], with particularly large gaps in certain structured environments (Section VI). Then, comparisons with state-of-the-art centralized and sequential methods (DFS-SG and DFS-BSG) under both idealized and realistic delay settings reveal a fundamental trade-off between coordination optimality and convergence speed, and highlight the importance of delay-aware evaluation for real-time performance. Although the benchmarks require relaxed versions of the problem in eq. (1) to be applicable, ANACONDA still achieves competitive or better coverage (Sections VII-A to VII-C). Finally, large-scale simulations confirm the scalability of ANACONDA: while benchmarks such as DFS-BSG incur prohibitive communication delays, ANACONDA maintains a constant time per decision round and can scale sublinearly in network size in practice (Section VII-D). We ran all simulations using Python 3.11.7 on a Windows PC with an Intel Core i9-14900KF CPU @ 3.20 GHz and 64 GB RAM. The code is available at <https://github.com/UM-iRaL/Self-configurable-network>.

Comparison with preliminary work [21], [43]. This paper extends our preliminary work [43] to include new theoretical results, extensive evaluations, and proofs of all claims. We introduce a tighter a priori bound (Theorem 1), a strictly positive a posteriori bound (Theorem 2), and a strictly positive asymptotic bound (Theorem 3), and we comprehensively evaluate the proposed algorithm across coordination performance, neighborhood design, and scalability metrics in area monitoring scenarios (Section VI). This paper also extends

the formulation in prior work [21] where communication neighborhoods are fixed and constructed heuristically (*e.g.*, via nearest neighbors). Here, we perform network optimization and demonstrate that the resulting configurations outperform nearest neighbors in area monitoring scenarios (Section VI).

II. DISTRIBUTED COORDINATION AND NETWORK CO-OPTIMIZATION

We present the problem formulation of *Distributed Coordination and Network Co-Optimization*. We use the notation:

- $\mathcal{V}_{\mathcal{N}} \triangleq \prod_{i \in \mathcal{N}} \mathcal{V}_i$ is the cross product of sets $\{\mathcal{V}_i\}_{i \in \mathcal{N}}$.
- $[T] \triangleq \{1, \dots, T\}$ for any positive integer T .
- $f(a | \mathcal{A}) \triangleq f(\mathcal{A} \cup \{a\}) - f(\mathcal{A})$ is the marginal gain of set function $f : 2^{\mathcal{V}} \mapsto \mathbb{R}$ for adding $a \in \mathcal{V}$ to $\mathcal{A} \subseteq \mathcal{V}$.
- $|\mathcal{A}|$ is the cardinality of a discrete set \mathcal{A} .

We also lay down the following framework about the agents' communication network and the objective function f .

Communication network. The agents' communication network $\mathcal{G}_t = (\mathcal{N}, \mathcal{E}_t)$, $\forall t$ is *undetermined* a priori, where \mathcal{E}_t is the set of (directed) communication edges among agents \mathcal{N} at time t . The goal of this work is for the agents to jointly optimize \mathcal{E}_t to enable convergence to a near-optimal solution to (1) despite distributed coordination. The network optimized by \mathcal{N} can be directed and even disconnected. We refer to the case where every agent receives information from all others as *fully centralized*, and the case where no agent receives information from any other as *fully decentralized*.

Communication neighborhood. When a communication channel exists from agent j to agent i at time t , *i.e.*, $(j \rightarrow i) \in \mathcal{E}_t$, then i can receive, store, and process information sent by j , and the set of all such j is i 's *communication neighborhood*, denoted as $\mathcal{N}_{i,t}$.

Communication constraints. Each agent i can receive information from up to α_i other agents at the same time due to onboard bandwidth constraints, *i.e.*, $|\mathcal{N}_{i,t}| \leq \alpha_i$, $\forall t$. Also, we denote as $\mathcal{M}_i \subseteq \mathcal{N} \setminus \{i\}$ the set of agents that can potentially send information to agent i —not all $\mathcal{N} \setminus \{i\}$ can reach agent i due to distance or obstacles: agent i can pick its neighbors by choosing at most α_i agents from \mathcal{M}_i . We refer to \mathcal{M}_i as agent i 's *coordination neighborhood* ($\mathcal{N}_{i,t} \subseteq \mathcal{M}_i$, $\forall t$).

Definition 1 (Normalized and Non-Decreasing Submodular Set Function [22]). *A set function $f : 2^{\mathcal{V}} \mapsto \mathbb{R}$ is normalized and non-decreasing submodular if and only if*

- (Normalization) $f(\emptyset) = 0$;
- (Monotonicity) $f(\mathcal{A}) \leq f(\mathcal{B})$, $\forall \mathcal{A} \subseteq \mathcal{B} \subseteq \mathcal{V}$;
- (Submodularity) $f(s | \mathcal{A}) \geq f(s | \mathcal{B})$, $\forall \mathcal{A} \subseteq \mathcal{B} \subseteq \mathcal{V}$ and $s \in \mathcal{V}$.

Intuitively, if $f(\mathcal{A})$ captures the number of targets tracked by a set \mathcal{A} of sensors, then the more sensors are deployed, more or the same targets are covered; this is the non-decreasing property. Also, the marginal gain of tracked targets caused by deploying a sensor s drops when more sensors are already deployed; this is the submodularity property.

Definition 2 (2nd-order Submodular Set Function [44], [45]). *$f : 2^{\mathcal{V}} \mapsto \mathbb{R}$ is 2nd-order submodular if and only if*

$$f(s | \mathcal{C}) - f(s | \mathcal{A} \cup \mathcal{C}) \geq f(s | \mathcal{B} \cup \mathcal{C}) - f(s | \mathcal{A} \cup \mathcal{B} \cup \mathcal{C}), \quad (2)$$

Algorithm 1: AlterNating COordination and Network Design Algorithm (ANACONDA) for Agent i

Input: Time horizon T ; agent i 's coordination neighborhood \mathcal{M}_i ; agent i 's communication bandwidth α_i .

Output: Action $a_{i,t}$ and communication neighborhood $\mathcal{N}_{i,t}$, $\forall t \in [T]$.

- 1: $\mathcal{N}_{i,0} \leftarrow \emptyset, \forall i \in \mathcal{N}$;
 - 2: **for** each time step $t \in [T]$ **do**
 - 3: $a_{i,t} \leftarrow \text{ACTSEL}([T], \mathcal{V}_i)$;
 - 4: $\mathcal{N}_{i,t} \leftarrow \text{NEISEL}(a_{i,t}, [T], \mathcal{M}_i, \alpha_i)$;
 - 5: **receive** neighbors' actions $\{a_{j,t}\}_{j \in \mathcal{N}_{i,t}}$ and **update** ACTSEL (per lines 6-8) and NEISEL (per lines 6-11);
 - 6: **end for**
-

for any disjoint $\mathcal{A}, \mathcal{B}, \mathcal{C} \subseteq \mathcal{V}$ ($\mathcal{A} \cap \mathcal{B} \cap \mathcal{C} = \emptyset$) and $s \in \mathcal{V}$.

Intuitively, if $f(\mathcal{A})$ captures the number of targets tracked by a set \mathcal{A} of sensors, then *marginal gain of the marginal gains* drops when more sensors are already deployed.

Problem 1 (Distributed Coordination and Network Co-Optimization). *At each $t \in [T]$, each agent $i \in \mathcal{N}$ selects a communication neighborhood $\mathcal{N}_{i,t}$ of size up to α_i and an action $a_{i,t}$ to solve the optimization problem*

$$\max_{\substack{\mathcal{N}_{i,t} \subseteq \mathcal{M}_i, |\mathcal{N}_{i,t}| \leq \alpha_i \\ \forall i \in \mathcal{N}, \forall t \in [T]}} \max_{\substack{a_{i,t} \in \mathcal{V}_i \\ \forall i \in \mathcal{N}, \forall t \in [T]}} \sum_{t=1}^T f(\{a_{i,t}\}_{i \in \mathcal{N}}), \quad (3)$$

where (i) each agent i can coordinate with its neighbors only, without any information about non-neighbors, (ii) $f: 2^{\mathcal{V}} \mapsto \mathbb{R}$ is a normalized, non-decreasing submodular, and 2nd-order submodular, and (iii) f is known via bandit feedback, in particular, each agent i can access the value of $f(\mathcal{A}_t)$ only, $\forall \mathcal{A}_t \subseteq \{a_{i,t}\} \cup \{a_{j,t}\}_{j \in \mathcal{N}_{i,t}}$, once the agent has selected $a_{i,t}$ and received $\{a_{j,t}\}_{j \in \mathcal{N}_{i,t}}$ from neighbors.

Problem 1 captures the intrinsic coupling between coordination performance and information access, as illustrated by the example in Figure 1. The objective of this paper is to design the communication network topology that maximizes action coordination performance through solving Problem 1.

III. ALTERNATING COORDINATION AND NETWORK-DESIGN ALGORITHM (ANACONDA)

We present ANACONDA. ANACONDA approximates a solution to Problem 1 by alternating the optimization for action coordination and communication neighborhood design. Since both action coordination and communication neighborhood design take the form of adversarial bandit problems, we present first the adversarial bandit (Section III-A), then the algorithms ACTSEL (Section III-B) and NEISEL (Section III-C).

A. Adversarial Bandit Problem

The adversarial bandit problem involves an agent selecting a sequence of actions to maximize the total reward over a given number of time steps [10]. The challenge is that, at each time step, no action's reward is known to the agent a priori, and

Algorithm 2: ACTSEL for Agent i

Input: Time horizon T and agent i 's action set \mathcal{V}_i .

Output: Agent i 's action $a_{i,t}$, $\forall t \in [T]$.

- 1: $\eta_i^a \leftarrow \sqrt{2 \log |\mathcal{V}_i| / (|\mathcal{V}_i| T)}$;
 - 2: $w_1 \leftarrow [w_{1,1}, \dots, w_{|\mathcal{V}_i|,1}]^\top$ with $w_{v,1} = 1, \forall a \in \mathcal{V}_i$;
 - 3: **for** each time step $t \in [T]$ **do**
 - 4: **get** distribution $p_t \leftarrow w_t / \|w_t\|_1$;
 - 5: **draw** action $a_{i,t} \in \mathcal{V}_i$ **from** p_t ;
 - 6: **input** $a_{i,t}$ **to** NEISEL and **receive** neighbors' actions $\{a_{j,t}\}_{j \in \mathcal{N}_{i,t}}$;
 - 7: $r_{a_{i,t},t} \leftarrow f(a_{i,t} | \{a_{j,t}\}_{j \in \mathcal{N}_{i,t}})$ and **normalize** $r_{a_{i,t},t}$ **to** $[0, 1]$;
 - 8: $\hat{r}_{a,t} \leftarrow 1 - \frac{\mathbf{1}(a_{i,t}=a)}{p_{a,t}} (1 - r_{a_{i,t},t}), \forall a \in \mathcal{V}_i$;
 - 9: $w_{a,t+1} \leftarrow w_{a,t} \exp(\eta_i^a \hat{r}_{a,t}), \forall a \in \mathcal{V}_i$;
 - 10: **end for**
-

after an action is selected, only the selected action's reward will become known. To present the problem, we have:

- \mathcal{V} denotes the available action set;
- $v_t \in \mathcal{V}$ denotes the agent's selected action at time t ;
- $r_{v_t,t} \in [0, 1]$ denotes the reward of selecting v_t at time t .

Problem 2 (Adversarial Bandit [10]). *Assume a horizon of T time steps. At each time step $t \in [T]$, the agent needs to select an action $v_t \in \mathcal{V}$ such that the regret*

$$\text{Regret}_T \triangleq \max_{v \in \mathcal{V}} \sum_{t=1}^T r_{v,t} - \sum_{t=1}^T r_{v_t,t}, \quad (4)$$

is minimized, where no actions' rewards are known a priori, and only the reward $r_{v_t,t} \in [0, 1]$ becomes known to the agent after v_t is selected.

The goal of solving Problem 2 is to achieve a sublinear Regret_T , i.e., $\text{Regret}_T/T \rightarrow 0$ for $T \rightarrow \infty$, since this implies that the agent asymptotically chooses optimal actions even though the rewards are unknown a priori [10]. The most classical adversarial bandit algorithm EXP3 [46] achieves the goal above by obtaining a regret bound of $\tilde{O}(\sqrt{|\mathcal{V}|T})$, where $\tilde{O}(\cdot)$ hides log terms. During the past two decades, several refined adversarial bandit algorithms have emerged, including EXP3-IX for high-probability regret bounds via implicit exploration [47], EXP3++ for adaptation between stochastic and adversarial regimes [48], and TSALLIS-INF for minimax-optimal regret with improved adaptivity through Tsallis entropy regularization [49].

In this paper, we will formulate both action coordination and neighbor selection problems in the form of Problem 2, and employ EXP3 as the bandit solver without loss of generality. Alternative methods such as those mentioned above are also applicable (e.g., EXP3-IX was used in [43]).

B. Action Coordination

We introduce the ACTSEL algorithm and establish its performance guarantees. To this end, we first define the coordination problem that ACTSEL addresses and relate it to Problem 2 for each agent.

- $\mathcal{A}_t \triangleq \{a_{i,t}\}_{i \in \mathcal{N}}$ is the set of all agents' actions at t ;
- $\mathcal{A}^{\text{OPT}} \in \arg \max_{a_i \in \mathcal{V}_i, \forall i \in \mathcal{N}} f(\{a_i\}_{i \in \mathcal{N}})$ is the optimal actions for agents \mathcal{N} that solve eq. (1).

Intuitively, each agent i 's goal at each time step t is to efficiently select an action $a_{i,t}$ that solves

$$\max_{a_{i,t} \in \mathcal{V}_i} f(a_{i,t} | \{a_{j,t}\}_{j \in \mathcal{N}_{i,t}}), \quad (5)$$

To enable efficiency, the agents should ideally select actions *simultaneously*, unlike offline algorithms such as Sequential Greedy [22] and Resource-Aware distributed Greedy [21] that employ (partially parallelized) sequential operations. But if they want to select actions simultaneously, $\{a_{j,t}\}_{j \in \mathcal{N}_{i,t}}$ will become known only after agent i selects $a_{i,t}$ and communicates with $\mathcal{N}_{i,t}$. Therefore, computing the marginal gain is possible only in hindsight, once all agents' decisions have been finalized for time step t . Thus, action selection for each agent aligns with the framework of Problem 2, where the reward of selecting $a_{i,t} \in \mathcal{V}_i$ is $r_{a_{i,t},t} \triangleq f(a_{i,t} | \{a_{j,t}\}_{j \in \mathcal{N}_{i,t}})$, which becomes available only after choosing $a_{i,t}$.

ACTSEL starts by initializing a learning rate η_i^a and a weight vector w_t for all available actions $a \in \mathcal{V}_i$ (Algorithm 2's lines 1-2). Then, at each $t \in [T]$, it sequentially executes the following steps:

- 1) Compute probability distribution p_t using w_t (lines 3-4);
- 2) Select action $a_{i,t} \in \mathcal{V}_i$ by sampling from p_t (line 5);
- 3) Send $a_{i,t}$ to NEISEL and receive neighbors' actions $\{a_{j,t}\}_{j \in \mathcal{N}_{i,t}}$ (line 6);
- 4) Compute reward $r_{a_{i,t},t}$, estimate reward $\hat{r}_{a_{i,t}}$ of each $a \in \mathcal{V}$, and update weight $w_{a,t+1}$ of each $a \in \mathcal{V}_i$ (lines 7-9).³

We introduce the novel quantification that evaluates the benefit of information access in solving Problem 1.

Definition 3 (Value of Coordination (VoC)). *Consider $t \in [T]$ and agent $i \in \mathcal{N}$ with action $a_{i,t}$ and coordination neighborhood \mathcal{M}_i . Agent i 's Value of Coordination is defined as:*

$$\text{VoC}_{f,t}(a_{i,t}; \mathcal{N}_{i,t}) \triangleq f(a_{i,t}) - f(a_{i,t} | \{a_{j,t}\}_{j \in \mathcal{N}_{i,t}}), \quad (6)$$

where $\mathcal{N}_{i,t} \subseteq \mathcal{M}_i$ is the communication neighborhood that i chooses to receive information from, $|\mathcal{N}_{i,t}| \leq \alpha_i$.

$\text{VoC}_{f,t}(a_{i,t}; \mathcal{N}_{i,t})$ is thus an information theory metric similar to mutual information yet over the set function f . It represents the overlap between agent i and its communication neighbors' actions. Particularly, $\sum_{t=1}^T \text{VoC}_{f,t}(a_{i,t}; \mathcal{N}_{i,t})$ evaluates agent i 's benefit in coordinating with $\mathcal{N}_{i,t}$ over the horizon T . The larger is this value, the more related is the received information to the selected actions.

Definition 4 (Curvature [50]). *The curvature of a normalized submodular function $f: 2^{\mathcal{V}} \mapsto \mathbb{R}$ is defined as*

$$\kappa_f \triangleq 1 - \min_{v \in \mathcal{V}} \frac{f(\mathcal{V}) - f(\mathcal{V} \setminus \{v\})}{f(v)}. \quad (7)$$

³The coordination algorithms in [18]–[20] instruct the agents to select actions simultaneously at each time step as ACTSEL, but they lift the coordination problem to the continuous domain and require each agent to know/estimate the gradient of the multilinear extension of f , which leads to a decision time at least one order higher than ACTSEL [21].

Algorithm 3: NEISEL for Agent i

Input: Time horizon T ; agent i 's coordination neighborhood \mathcal{M}_i ; agent i 's communication bandwidth α_i .

Output: Agent i 's communication neighborhood $\mathcal{N}_{i,t}$, $\forall t \in [T]$.

- 1: $\eta_i^n \leftarrow \sqrt{2 \log |\mathcal{M}_i| / (|\mathcal{M}_i| T)}$;
 - 2: $z_1^{(k)} \leftarrow [z_{1,1}^{(k)}, \dots, z_{\alpha_i,1}^{(k)}]^\top$ with $z_{j,1}^{(k)} = 1$, $\forall v \in \mathcal{M}_i, \forall k \in [\alpha_i]$;
 - 3: **for** each time step $t \in [T]$ **do**
 - 4: **receive** action $a_{i,t}$ **from** ACTSEL;
 - 5: **for** $k = 1, \dots, \alpha_i$ **do**
 - 6: **get** distribution $q_t^{(k)} \leftarrow z_t^{(k)} / \|z_t^{(k)}\|_1$;
 - 7: **draw** agent $j_t^{(k)} \in \mathcal{M}_i$ **from** $q_t^{(k)}$;
 - 8: **receive** action $a_{j_t^{(k)},t}$ **from** $j_t^{(k)}$;
 - 9: $r_{j_t^{(k)},t} \leftarrow \text{VoC}_{f,t}(a_{i,t}; \{a_{j_t^{(1)},t}, \dots, a_{j_t^{(k)},t}\}) - \text{VoC}_{f,t}(a_{i,t}; \{a_{j_t^{(1)},t}, \dots, a_{j_t^{(k-1)},t}\})$
and **normalize** $r_{j_t^{(k)},t}$ **to** $[0, 1]$;
 - 10: $\hat{r}_{j_t^{(k)},t} \leftarrow 1 - \frac{\mathbf{1}(j_t^{(k)}=j)}{q_{j,t}^{(k)}} \left(1 - r_{j_t^{(k)},t}\right)$, $\forall j \in \mathcal{M}_i$;
 - 11: $z_{j,t+1}^{(k)} \leftarrow z_{j,t}^{(k)} \exp(\eta_i^n \hat{r}_{j,t}^{(k)})$, $\forall j \in \mathcal{M}_i$;
 - 12: **end for**
 - 13: $\mathcal{N}_{i,t} \leftarrow \{j_{k,t}\}_{k \in [\alpha_i]}$;
 - 14: **end for**
-

Intuitively, κ_f measures how far f is from modularity: if $\kappa_f = 0$, then $f(\mathcal{V}) - f(\mathcal{V} \setminus \{v\}) = f(v)$, $\forall v \in \mathcal{V}$, i.e., f is modular. In contrast, $\kappa_f = 1$ in the extreme case where there exist $v \in \mathcal{V}$ such that $f(\mathcal{V}) = f(\mathcal{V} \setminus \{v\})$, i.e., v has no contribution in the presence of $\mathcal{V} \setminus \{v\}$.

Proposition 1 (Approximation Performance of ACTSEL). *Over $t \in [T]$, agents \mathcal{N} can use ACTSEL to select actions $\{\mathcal{A}_t\}_{t \in [T]}$ such that*

$$\sum_{t=1}^T f(\mathcal{A}_t) \geq (1 - \kappa_f) \sum_{t=1}^T \left[f(\mathcal{A}^{\text{OPT}}) + \sum_{i \in \mathcal{N}} \text{VoC}_{f,t}(a_{i,t}; \mathcal{N}_{i,t}) \right] - \tilde{O} \left(|\mathcal{N}| \sqrt{|\bar{\mathcal{V}}| T} \right). \quad (8)$$

where $|\bar{\mathcal{V}}| \triangleq \max_{i \in \mathcal{N}} |\mathcal{V}_i|$.

Proposition 1 implies that ACTSEL's performance increases for neighborhoods $\{\mathcal{N}_{i,t}\}_{i \in \mathcal{N}}$ with higher $\text{VoC}_{f,t}(a_{i,t}; \mathcal{N}_{i,t})$. The proof appears in Appendix A.

Lemma 1 (Monotonicity and Submodularity of VoC). *Given an action $a \in \mathcal{V}_i$ and a non-decreasing and 2nd-order submodular function $f: 2^{\mathcal{V}} \mapsto \mathbb{R}$, then $\text{VoC}_{f,t}(a; \cdot)$ is non-decreasing and submodular in the second argument.*

NEISEL will next leverage Lemma 1 to enable each agent to individually select its communication neighborhood that optimizes the approximation bound of ACTSEL (Proposition 1).

C. Neighbor Selection

We now present the NEISEL algorithm and its performance guarantees for maximizing VoC. Particularly, we introduce

the neighbor-selection problem that NEISEL enables agents to solve in parallel and demonstrate that it aligns with Problem 2.

Since the suboptimality bound of ACTSEL in eq. (8) improves as $\text{VoC}_{f,t}(a_{i,t}; \mathcal{N}_{i,t})$ increases, NEISEL aims to enable each agent i to choose neighbors by solving the following cardinality-constrained maximization problem:

$$\max_{\mathcal{N}_{i,t} \subseteq \mathcal{M}_i, |\mathcal{N}_{i,t}| \leq \alpha_i} \sum_{t=1}^T \text{VoC}_{f,t}(a_{i,t}; \mathcal{N}_{i,t}), \quad (9)$$

where $a_{i,t}$ is given by ACTSEL. This is a submodular maximization problem since we show in Lemma 1 that $\text{VoC}_{f,t}(a_{i,t}; \mathcal{N}_{i,t})$ is submodular in $\mathcal{N}_{i,t}$. But $\text{VoC}_{f,t}(a_{i,t}; \mathcal{N}_{i,t})$ is computable in hindsight only: $\{a_{j,t}\}_{j \in \mathcal{N}_{i,t}}$ become known only after agent i has selected and communicated with $\mathcal{N}_{i,t}$. Therefore, eq. (9) takes the form of cardinality-constrained bandit submodular maximization [1], [32], [51], which is an extension of Problem 2 to the multi-agent submodular setting.

Solving eq. (9) using algorithms for Problem 2 will lead to exponentially large \mathcal{V} per eq. (4) [51]. Therefore, NEISEL instead extends [51, Algorithm 2], which can solve eq. (9) in the full-information setting, to the bandit setting [1]. Specifically, NEISEL decomposes eq. (9) to α_i instances of Problem 2, and separately solves each of them using EXP3.

NEISEL starts by initializing a learning rate η_i^n and α_i weight vectors $z_t^{(k)}, \forall k \in [\alpha_i]$, each determining the k -th selection in $\mathcal{N}_{i,t}$ (Algorithm 3's lines 1-2). Then, at each $t \in [T]$, it sequentially executes the following steps:

- 1) Receive action $a_{i,t}$ by ACTSEL (lines 3-4);
- 2) Compute distribution $q_t^{(k)}$ using $z_t^{(k)}, \forall k \in [\alpha_i]$ (lines 5-6);
- 3) Select agent $j_t^{(k)} \in \mathcal{M}_i$ as neighbor by sampling from $q_t^{(k)}$, and receive its action $a_{j_t^{(k)},t}, \forall k \in [\alpha_i]$ (lines 7-8);
- 4) For each $k \in [\alpha_i]$, compute reward $r_{j_t^{(k)},t}$ associated with each $j_t^{(k)}$, estimate reward $\tilde{r}_{j_t^{(k)},t}^{(k)}$ of each $j \in \mathcal{M}_i$, and update weight $z_{j,t+1}^{(k)}$ of each $j \in \mathcal{M}_i$ (lines 9-12).

IV. SUBOPTIMALITY GUARANTEES

We show that ANACONDA's approximation performance against the optimal solution to eq. (1) improves with the sum of all agents' VoC, and is strictly positive anytime, even before convergence. To this end, we begin with an a priori bound validating that NEISEL indeed improves ANACONDA's performance bound (Section IV-A). We then provide an anytime strictly positive a posteriori bound (Section IV-B). Combining the first two results, we finally present an asymptotic bound (Section IV-C). All proofs appear in Appendix A.

A. A Priori Bound

To present the a priori bound, we first present the following definitions and lemmas that measure the performances of ACTSEL and NEISEL. We use the following notation:

- $\kappa_{I,i} \triangleq \max_{t \in [T]} \kappa_{I,i,t}$, where $\kappa_{I,i,t}$ is the curvature of $\text{VoC}_{f,t}(a_{i,t}; \cdot), \forall t \in [T]$. $\kappa_{I,i}$ is independent of κ_f ;

- $\rho(\kappa, \alpha) \triangleq \kappa^{-1} [1 - (1 - \kappa/\alpha)^\alpha]$, where $\kappa \in [0, 1]$ and $\alpha \in \mathbb{N}$. Notice that $1 \geq \kappa^{-1} [1 - (1 - \kappa/\alpha)^\alpha] \stackrel{\alpha \rightarrow \infty}{>} \kappa^{-1} (1 - e^{-\kappa}) \stackrel{\kappa \rightarrow 1}{\geq} 1 - e^{-1}$.

The performances of ACTSEL and NEISEL are measured by the following quantities:

Definition 5 (Static Regret of Action Selection). *Given agent i has neighbors $\{\mathcal{N}_{i,t}\}_{t \in [T]}$ over the horizon $[T]$. At each time step t , suppose agent i selects an action $a_{i,t}$. Then, the static regret of $\{a_{i,t}\}_{t \in [T]}$ is defined as*

$$\begin{aligned} \text{A-Reg}_T(\{a_{i,t}\}_{t \in [T]}) &\triangleq \\ \max_{a \in \mathcal{V}_i} \sum_{t=1}^T f(a | \{a_{j,t}\}_{j \in \mathcal{N}_{i,t}}) &- \sum_{t=1}^T f(a_{i,t} | \{a_{j,t}\}_{j \in \mathcal{N}_{i,t}}). \end{aligned} \quad (10)$$

Definition 6 ($\rho(\kappa_{I,i}, \alpha_i)$ -Approximate Static Regret of Neighbor Selection). *Given agent i has actions $\{a_{i,t}\}_{t \in [T]}$ over horizon $[T]$. At each time step t , suppose agent i selects a set of neighbors $\mathcal{N}_{i,t} \subseteq \mathcal{M}_i, |\mathcal{N}_{i,t}| \leq \alpha_i$. Then, the $\rho(\kappa_{I,i}, \alpha_i)$ -approximate static regret of $\{\mathcal{N}_{i,t}\}_{t \in [T]}$ is defined as*

$$\begin{aligned} \text{N-Reg}_{\{a_{i,t}\}_{t \in [T]}}^{\rho(\kappa_{I,i}, \alpha_i)}(\{\mathcal{N}_{i,t}\}_{t \in [T]}) & \\ \triangleq \rho(\kappa_{I,i}, \alpha_i) \max_{\mathcal{N}_{i,t} \subseteq \mathcal{M}_i, |\mathcal{N}_{i,t}| \leq \alpha_i} \sum_{t=1}^T \text{VoC}_{f,t}(a_{i,t}; \mathcal{N}_{i,t}) & \\ - \sum_{t=1}^T \text{VoC}_{f,t}(a_{i,t}; \mathcal{N}_{i,t}). & \end{aligned} \quad (11)$$

Definition 6 evaluates the suboptimality of $\{\mathcal{N}_{i,t}\}_{t \in [T]}$ against the optimal communication neighborhood that would have been selected if $\text{VoC}_{f,t}(a_{i,t}; \cdot)$ had been known a priori, $\forall t \in [T]$. The optimal value in eq. (11) is discounted by $\rho(\kappa_{I,i}, \alpha_i)$ since the problem in eq. (9) is NP-hard to solve with an approximation factor greater than $\rho(\kappa_{I,i}, \alpha_i)$ even when $\text{VoC}_{f,t}(a_{i,t}; \cdot)$ is known a priori [50].

Lemma 2 (Suboptimality Guarantee of ACTSEL). *Consider horizon $[T]$. If agent i has a sequence of neighbors $\{\mathcal{N}_{i,t}\}_{t \in [T]}$, regardless of how they are selected, then using ACTSEL, agent i can choose actions $\{a_{i,t}\}_{t \in [T]}$ such that*

$$\text{A-Reg}_T(\{a_{i,t}\}_{t \in [T]}) \leq \tilde{O}\left(\sqrt{|\mathcal{V}_i|T}\right), \quad (12)$$

given the learning rate is set as $\eta_i^n = \sqrt{2 \log |\mathcal{V}_i| / (|\mathcal{V}_i|T)}$.

Lemma 3 (Suboptimality Guarantee of NEISEL). *Consider horizon $[T]$. If agent i has a sequence of actions $\{a_{i,t}\}_{t \in [T]}$, regardless of how they are selected, then using NEISEL, agent i can choose neighbors $\{\mathcal{N}_{i,t}\}_{t \in [T]}$ such that*

$$\text{N-Reg}_{\{a_{i,t}\}_{t \in [T]}}^{\rho(\kappa_{I,i}, \alpha_i)}(\{\mathcal{N}_{i,t}\}_{t \in [T]}) \leq \tilde{O}\left(\alpha_i \sqrt{|\mathcal{M}_i|T}\right), \quad (13)$$

given the learning rate set as $\eta_i^n = \sqrt{2 \log |\mathcal{M}_i| / (|\mathcal{V}_i|T)}$.

Now we present the a priori bound of ANACONDA.

Theorem 1 (A Priori Approximation Performance). *Using ANACONDA, each agent i selects actions $\{a_{i,t}\}_{t \in [T]}$ and*

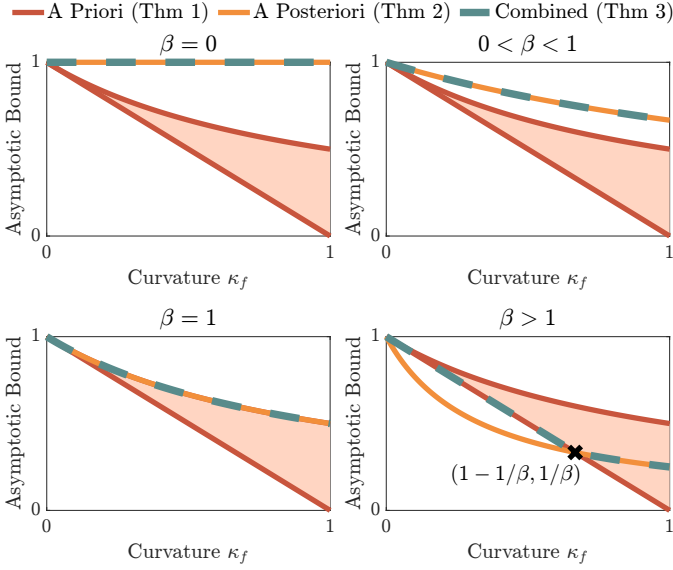


Fig. 2: **Asymptotic approximation bounds of ANACONDA.** As $T \rightarrow \infty$, the bounds provided by Theorems 1 to 3 are shown with varying ranges of κ_f and achieved β (defined in eq. (18)). The a priori bound (red) varies with the sum of all agents' VoC; the a posteriori bound (orange) decreases as β increases; and the combined bound (green) takes the maximum of the a priori lower bound and the a posteriori bound.

communication neighborhoods $\{\mathcal{N}_{i,t}\}_{t \in [T]}$ that guarantee:

$$\begin{aligned} \mathbb{E}[f(\mathcal{A}_t)] &\geq (1 - \kappa_f) f(\mathcal{A}^{\text{OPT}}) \\ &+ \kappa_f (1 - \kappa_f) \rho(\kappa_I, \bar{\alpha}) \\ &\times \sum_{i \in \mathcal{N}} \mathbb{E}[\text{VoC}_{f,t}(a_{i,t}; \mathcal{N}_i^*(\{a_{i,t}\}_{t \in [T]}; \alpha_i, \mathcal{M}_i))] \\ &- \tilde{O}\left(|\mathcal{N}| \sqrt{(\bar{\alpha}^2 |\bar{\mathcal{M}}| + |\bar{\mathcal{V}}|)/T}\right), \end{aligned} \quad (14)$$

where $\kappa_I \triangleq \max_{i \in \mathcal{N}} \kappa_{I,i}$, $\bar{\alpha} \triangleq \max_{i \in \mathcal{N}} \alpha_i$, $|\bar{\mathcal{V}}| \triangleq \max_{i \in \mathcal{N}} |\mathcal{V}_i|$, $|\bar{\mathcal{M}}| \triangleq \max_{i \in \mathcal{N}} |\mathcal{M}_i|$, $\kappa_f, \kappa_I \in [0, 1]$, $\rho(\kappa_I, \bar{\alpha}) \in [1 - 1/e, 1]$, and $\mathcal{N}_i^*(\{a_{i,t}\}_{t \in [T]}; \alpha_i, \mathcal{M}_i) \subseteq \mathcal{M}_i$ is the optimal communication neighborhood that solves eq. (9) given $\{a_{i,t}\}_{t \in [T]}$ subject to α_i . The expectation is due to the algorithm's internal randomness.

Theorem 1 implies that as $T \rightarrow \infty$, the a priori approximation ratio spans the interval between fully centralized and fully decentralized coordination in accordance to VoC, and the spectrum is depicted in red in Fig. 2. In particular, when the network is fully centralized with all agents listening to all others, i.e., $\mathcal{N}_{i,t} \equiv \mathcal{N} \setminus \{i\}$,

$$\mathbb{E}[f(\mathcal{A}_t)] \geq \frac{1}{1 + \kappa_f} f(\mathcal{A}^{\text{OPT}}) - \tilde{O}\left(|\mathcal{N}| \sqrt{|\bar{\mathcal{V}}|/T}\right), \quad (15)$$

where the guaranteed $1/(1 + \kappa_f)$ bound is near-optimal [50]. When the network is fully decentralized with no agent listening to any others, i.e., $\mathcal{N}_{i,t} \equiv \emptyset$,

$$\mathbb{E}[f(\mathcal{A}_t)] \geq (1 - \kappa_f) f(\mathcal{A}^{\text{OPT}}) - \tilde{O}\left(|\mathcal{N}| \sqrt{|\bar{\mathcal{V}}|/T}\right), \quad (16)$$

where $1 - \kappa_f$ is the worst-case bound achieved by ANACONDA.

B. A Posteriori Bound

We provide an a posteriori bound for ANACONDA that is strictly positive, even for finite T .

Theorem 2 (A Posteriori Approximation Performance). Using ANACONDA, each agent $i \in \mathcal{N}$ selects $\{a_{i,t}\}_{t \in [T]}$ and $\{\mathcal{N}_{i,t}\}_{t \in [T]}$ that guarantee:

$$\mathbb{E}[f(\mathcal{A}_t)] \geq \frac{1}{1 + \beta \kappa_f + \tilde{O}\left(|\mathcal{N}| \sqrt{|\bar{\mathcal{V}}|/T}\right)} f(\mathcal{A}^{\text{OPT}}), \quad (17)$$

where

$$\beta \triangleq \frac{\mathbb{E}\left[\sum_{i \in \mathcal{N}} f(a_{i,t} | \{a_{j,t}\}_{j \in \mathcal{N}_{i,t}})\right]}{\mathbb{E}[f(\mathcal{A}_t)]} \in [0, \infty) \quad (18)$$

is computable after ANACONDA terminates. The expectation is due to the algorithm's internal randomness.

The bound is depicted in Fig. 2 in orange for varying ranges of β . Since $\mathbb{E}[f(\mathcal{A}_t)] > 0$, then $\beta < \infty$, and Theorem 2 implies that ANACONDA always achieves a strictly positive asymptotic approximation ratio:

$$\mathbb{E}[f(\mathcal{A}_t)] \stackrel{T \rightarrow \infty}{\geq} \frac{1}{1 + \beta \kappa_f} f(\mathcal{A}^{\text{OPT}}) > 0. \quad (19)$$

Moreover, if $\beta = 0$, i.e., each agent's selected action fully overlaps with its neighbors' selected actions, then ANACONDA is asymptotically optimal:

$$\mathbb{E}[f(\mathcal{A}_t)] \stackrel{T \rightarrow \infty}{\geq} f(\mathcal{A}^{\text{OPT}}). \quad (20)$$

Finally, if $0 \leq \beta \leq 1$, then ANACONDA asymptotically outperforms the bound of Sequential Greedy [22]:

$$\mathbb{E}[f(\mathcal{A}_t)] \stackrel{T \rightarrow \infty}{\geq} \frac{1}{1 + \beta \kappa_f} f(\mathcal{A}^{\text{OPT}}) \geq \frac{1}{1 + \kappa_f} f(\mathcal{A}^{\text{OPT}}). \quad (21)$$

This last scenario is guaranteed to occur when, e.g., there exists an order of the agents such that $[i - 1] \subseteq \mathcal{N}_{i,t}, \forall i, \forall t$.

C. Combined Asymptotic Bound

Combining Theorems 1 and 2, we get:

Theorem 3 (Asymptotic Approximation Performance). ANACONDA asymptotically achieves:

$$\frac{\mathbb{E}[f(\mathcal{A}_t)]}{f(\mathcal{A}^{\text{OPT}})} \stackrel{T \rightarrow \infty}{\geq} \max\left(1 - \kappa_f, \frac{1}{1 + \beta \kappa_f}\right) > 0, \quad (22)$$

where $\kappa_f \in [0, 1]$ and $\beta \in [0, \infty)$.

The bound is depicted in Fig. 2 in green.

V. DECISION TIME ANALYSIS

We present the convergence time of ANACONDA by analyzing its computation and communication complexity, accounting for the delays due to function evaluation and the transmission of messages under realistic communications.

- τ_f is the time required for one evaluation of f ;
- τ_c is the time for agent i to transmit the information about one action to agent j , without loss of generality, for all $(i \rightarrow j) \in \mathcal{E}_t, \forall t$.

Theorem 4 (Convergence Time). ANACONDA converges in $O[(\tau_f \bar{\alpha} + \tau_c)(\bar{\alpha}^2 |\bar{\mathcal{M}}| + |\bar{\mathcal{V}}|) |\mathcal{N}|^2 / \epsilon]$ time.

In sparse networks, the following corollary holds:

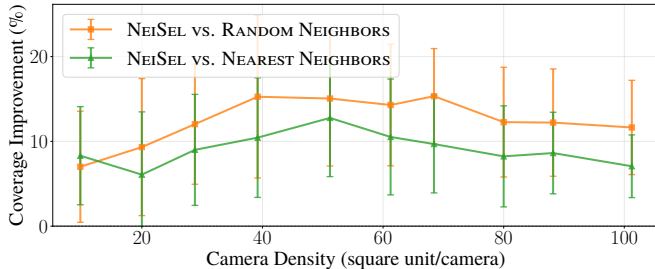


Fig. 3: **Comparison of neighbor selection strategies with varying network density.** Across 20 MC trials each with 2000 decision rounds, we compare NEISEL with two benchmark strategies, Nearest Neighbors and Random Neighbors. We tune the network density by varying the map area while fixing the network size at 20 agents: as the camera density grows, the network becomes sparser.

Corollary 1 (Convergence Time for Sparse Networks). *In sparse networks, where $|\mathcal{M}_i| = o(|\mathcal{N}|)$, $\forall i \in \mathcal{N}$, ANACONDA converges in $O[(\tau_f \bar{\alpha} + \tau_c) |\bar{\mathcal{V}}| |\mathcal{N}|^2 / \epsilon]$ time.*

The proof appears in Appendix B.

VI. NECESSITY FOR NETWORK OPTIMIZATION: NUMERICAL EVALUATION IN AREA MONITORING

In this section, we demonstrate that optimizing the network topology, per ANACONDA, leads to improved coordination performance compared to heuristics for network design, such as the nearest and random selection that are typically used in controls and robotics [21], [41], [42]. In particular, we compare the proposed NEISEL (Algorithm 3) with two heuristic strategies, *Nearest Neighbors* and *Random Neighbors*, in simulated 2D area-monitoring scenarios. The results show that NEISEL consistently outperforms the benchmarks across different network densities (Fig. 3), and that while nearest-neighbor heuristic is quite *misleading* in certain structured environments, NEISEL can configure the optimal communication neighborhood (Fig. 4). We defer the description of the former simulations to Appendix V and describe the latter below.

In more detail, eight cameras are deployed to monitor four street blocks as shown in Fig. 4. Under $\alpha_i = 1$ for all $i \in \mathcal{N}$, the optimal neighbor for each camera is the one positioned opposite its corresponding street block so as to minimize FOV overlap. The results, shown in Fig. 4 and Table I, indicate that NEISEL outperforms the two heuristic baselines by 27.2% and 11.5% in mean coverage, respectively. We next describe the simulation setup, compared algorithms, and results.

Setup. Environment: The environment is a 110×40 map with four 20×40 street blocks to monitor, as in Fig. 4. **Agents:** Eight cameras are located on the boundaries of street blocks with locations $(0, 20)$, $(20, 20)$, $(30, 20)$, $(50, 20)$, $(60, 20)$, $(80, 20)$, $(90, 20)$, and $(110, 20)$. They all have large enough communication ranges c_i such that $\mathcal{M}_i = \mathcal{N} \setminus \{i\}$, $\forall i \in \mathcal{N}$. **Actions:** All cameras $i \in \mathcal{N}$ have FOV radius $r_i = 20$ and AOV $\theta_i = \pi/2$, with direction $a_{i,t}$ chosen from the 16 cardinal directions, $\forall t$. Each camera i is considered unaware of \mathcal{V}_j , $j \in \mathcal{N} \setminus \{i\}$. Thus, the cameras have to communicate to know about one another’s action information. **Communication Network:** The emergent time-varying communication network \mathcal{G}_t can be directed and disconnected. At each decision round t , each camera i will first find its coordination neighborhood

TABLE I: Comparison of coverage performance (%) in the urban scenario as in Fig. 4 with different neighbor selection strategies. The best coverage performance is in **bold**.

Metric	Nearest Neighbors	Random Neighbors	Ours
Mean \pm Std (%)	56.53 \pm 4.57	64.47 \pm 6.07	71.89 \pm 7.36
Min (%)	35.56 ($t=1$)	37.94 ($t=113$)	39.72 ($t=169$)
Max (%)	71.09 ($t=2484$)	72.56 ($t=895$)	77.25 ($t=619$)

$\mathcal{M}_i \triangleq \{j\}_{\|x_j - x_i\| \leq c_i, j \in \mathcal{N} \setminus \{i\}}$, where c_i is i ’s communication range. Then, it will select communication neighborhood $\mathcal{N}_{i,t}$ from \mathcal{M}_i , following a strategy that will be determined by different compared algorithms. Once $\mathcal{N}_{i,t}$ is configured by all $i \in \mathcal{N}$, then \mathcal{G}_t is defined. **Objective Function:** $f(\{a_{i,t}\}_{i \in \mathcal{N}})$ is the total area of interest covered by the cameras \mathcal{N} when they select $\{a_{i,t}\}_{i \in \mathcal{N}}$ as their FOV directions. f is proved to be submodular [3].

Performance Metrics. We evaluate the achieved coverage of street blocks of the algorithms over 3000 decision rounds.

Compared Algorithms. We evaluate the following benchmarks, all selecting one neighbor per camera at each decision round, *i.e.*, $\alpha_i = 1$ for all $i \in \mathcal{N}$: (i) ANACONDA: Our algorithm will follow the process described in Section III. That is, at each round, the agents will each first sample its action $a_{i,t} \in \mathcal{V}_i$ per ACTSEL and neighbors $\mathcal{N}_{i,t} \subseteq \mathcal{M}_i$ per NEISEL. Then, they will each communicate with $\mathcal{N}_{i,t}$ and use the received information to update the two bandit algorithms. (ii) ACTSEL + *Nearest Neighbors*: Action selection follows ANACONDA, while each camera i will always have the same closest agent $j \in \mathcal{M}_i$ as its neighbor. (iii) ACTSEL + *Random Neighbors*: Action selection follows ANACONDA, while each camera i will uniformly resample its neighbor from \mathcal{M}_i at each decision round.

Results. We observe that network optimization via NEISEL increases both coverage performance and convergence speed, as shown in Fig. 4. In particular, ANACONDA outperforms the two benchmarks in all aspects of mean, minimum, and maximum coverage. It improves the benchmarks by $(71.89\%/56.53\% - 1) = 27.2\%$ and $(71.89\%/64.47\% - 1) = 11.5\%$ in the mean coverage, respectively (Table I). Moreover, NEISEL converges to the optimal network configuration after ~ 1000 rounds, and then ACTSEL also converges to the optimal coverage performance (77.25%) after ~ 1800 rounds (Fig. 4(c)). In contrast, we do not observe any convergence for the nearest neighbor selection (Fig. 4(a)), and the convergence appears slower for random neighbor selection after ~ 2400 rounds, with a suboptimal coverage performance (72.56%).

The reason why random neighbor selection performs better than nearest neighbor selection is that the latter will always select the same neighbors, thus never choose the optimal configuration. In contrast, random selection can happen to pick the optimum by chance, thus providing better performance.

VII. NUMERICAL EVALUATION IN AREA MONITORING

While much of the distributed optimization literature analyzes computation and communication complexities, it rarely considers how the resulting delays influence the algorithm’s practical optimality over time. In time-critical applications, however, the ability to make rapid decisions is essential, and

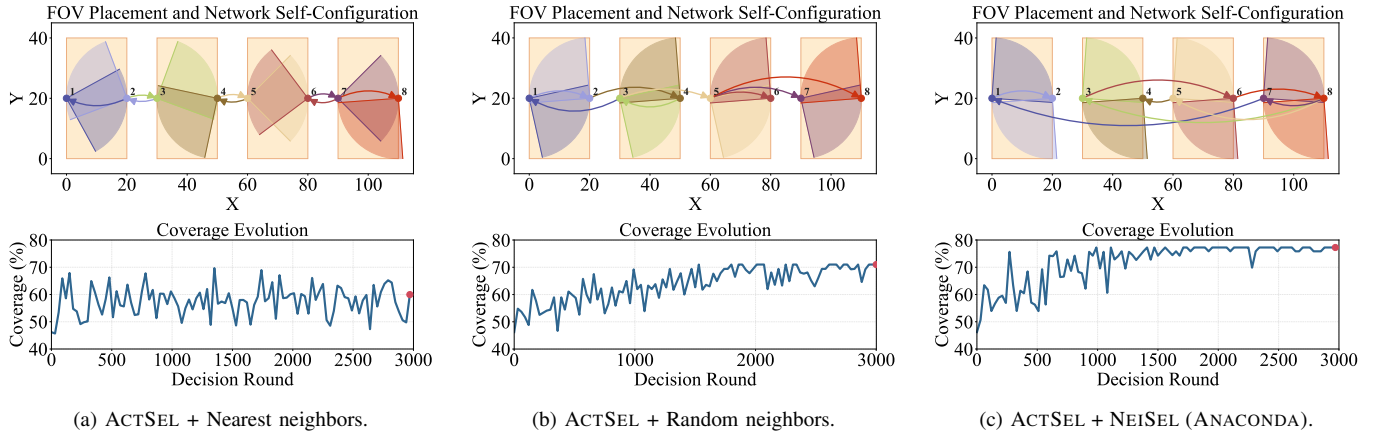


Fig. 4: **Comparison of neighbor selection strategies in a structured environment.** Three algorithms are compared with the same action selection strategy ACTSEL but different neighbor selection strategies (NEISEL vs. nearest neighbors vs. random neighbors) in the same structured environment.

computation and communication delays directly decide how many coordination rounds can be completed within a finite time horizon. As a result, an algorithm with a lower theoretical bound but higher decision frequency may outperform another with a higher bound but lower frequency, and thus delay-aware evaluation is crucial for revealing such effects.

To this end, in the section, we demonstrate the benefits of ANACONDA by comparing it with benchmarks under two settings, *i.e.*, with and without communication and computation delays. In particular, ANACONDA outperforms because it runs fast under delays. The simulation results, summarized in Figs. 5–7 and Table II, highlight the following insights:

- ANACONDA achieves competitive or improved performances to benchmarks, with and without delays, *even though the benchmarks are tasked with easier versions of the problem that ANACONDA solves and have higher performance bounds* (Sections VII-B to VII-D).
- ANACONDA is observed to scale sublinearly in $|\mathcal{N}|$ under delays, in contrast to the benchmark that has almost no benefit in network growth. (Section VII-D).

The common simulation setup is the same as Section VI. We next detail the benchmark algorithms (Section VII-A) and comparison results without delays (Section VII-B), with delays (Section VII-C), and scalability under delays (Section VII-D).

A. Compared Algorithms

We compare the following three algorithms.

a) *ANACONDA with different communication neighborhood sizes:* We test ANACONDA varying the maximum communication neighborhood size $|\mathcal{N}_{i,t}| \leq \alpha_i$, namely ANACONDA- $\alpha_i\mathcal{N}$, where $\alpha_i \in \{0, \dots, 5\}$.

b) *DFS-SG that requires a (strongly) connected network and a known environment [25]:* We test DFS-SG in terms of its achieved objective value after one round of multi-agent decisions. The offline algorithm is an implementation with communication specifications of SG for submodular maximization, which uses a DFS-based method to distributively determine the next agent over the (strongly) connected communication network. Therefore, the problem solved by DFS-SG is a relaxed version of Problem 1 where f is known and a connected communication network is given. DFS-SG

enjoys the same $1/(1 + \kappa_f)$ suboptimality bound as SG [22] and has a worst-case $O(\tau_c |\mathcal{N}|^3)$ decision time. The proof of decision time appears in Appendix C.

c) *DFS-BSG that requires a (strongly) connected network:* We test DFS-BSG in terms of its achieved objective value and convergence speed across multiple rounds of multi-agent decisions. The bandit algorithm is an implementation with communication specifications of BSG [1] that, similarly to ANACONDA, also decomposes multi-agent online decision-making into single-agent problems. But different from ANACONDA, per DFS-BSG, (i) each agent i 's action selection reward is $f(a_{i,t} | \{a_{j,t}\}_{j \in [i-1]})$ instead of $f(a_{i,t} | \{a_{j,t}\}_{j \in \mathcal{N}_{i,t}})$, $\forall t$, and (ii) computing rewards is enabled by the sequential communication over all agents in a DFS-based order.⁴ The problem solved by DFS-BSG is a relaxed version of Problem 1 where a connected communication network is given. DFS-BSG enjoys the same suboptimality bound as ANACONDA in the fully centralized case per Theorem 1, and thus upon convergence, DFS-BSG has the same guarantee as DFS-SG. It requires $O[(\tau_f |\mathcal{V}| |\mathcal{N}|^2 + \tau_c |\mathcal{N}|^5) |\mathcal{V}| / \epsilon]$ time to converge in a directed network. The proofs of suboptimality guarantees and decision time appear in Appendix D.

When implementing the algorithms above in each MC trial, we first let each agent i construct \mathcal{M}_i within the given communication range c_i . Then, while each agent actively selects neighbors $\mathcal{N}_{i,t} \subseteq \mathcal{M}_i$ with ANACONDA, it will directly take $\mathcal{N}_{i,t} \equiv \mathcal{M}_i, \forall t$ with DFS-SG and DFS-BSG. Although ANACONDA can accommodate arbitrary networks, we need to choose a not too small c_i to ensure the resulting network is connected for DFS-SG and DFS-BSG.

B. Comparison with No Delays: Coverage vs. Decision Round

To demonstrate the benefit of information access to the suboptimality of ANACONDA, we evaluate the above algorithms omitting computation and communication delays across four scenarios. (Fig. 5). Each scenario is assessed over 20 MC trials, where DFS-SG is executed for a single decision round and all other algorithms are run for 4000 rounds.

⁴In [1], the BSG algorithm uses EXP3*-SIX as the single-agent algorithm that provides bounded tracking regret in dynamic environments. In this paper, although we instead consider static regret and adopt EXP3, the sequential communication scheme and decision time of BSG are not altered.

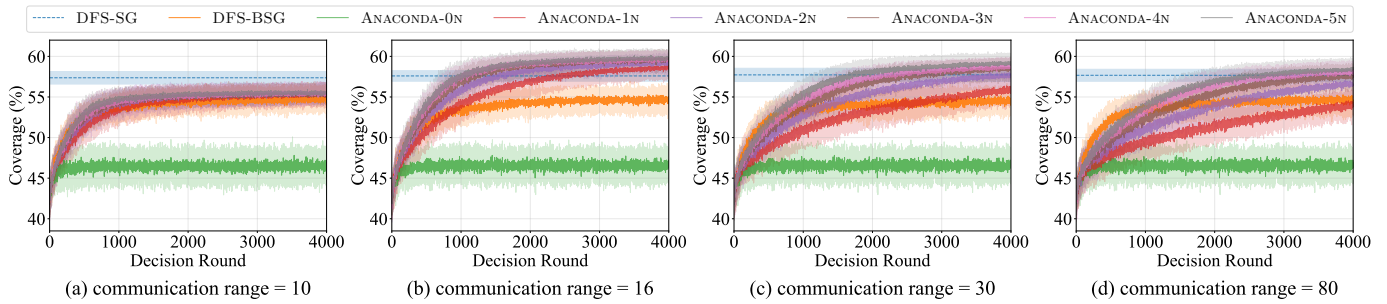


Fig. 5: **Comparison of ANACONDA, DFS-SG, and DFS-BSG for area monitoring without computation and communication delays.** Cameras select their FOV directions using ANACONDA with maximum communication neighborhood sizes in $\{0, \dots, 5\}$, or using DFS-SG or DFS-BSG. From (a) to (d), the communication range c_i for all cameras $i \in \mathcal{N}$ increases from 10 to 16 to 20 to 80, and thus expanding each camera’s coordination neighborhood \mathcal{M}_i growing from a small locality to the full set $\mathcal{N} \setminus i$. DFS-SG is executed for a single decision round, whereas the other algorithms are run for 4000 rounds. Results are averaged over 20 Monte Carlo trials.

Setup. Environment: A static 50×50 map. **Agents:** There exist 50 cameras. The communication ranges $c_i \in \{10, 16, 30, 80\}$ across the four scenarios. In each MC trial, the location x_i of each camera $i \in \mathcal{N}$ is uniformly sampled in $[0, 50]^2$. **Actions:** Direction $a_{i,t}$ is chosen from the 16 cardinal directions, $\forall t$, with FOV radius $r_i = 8$ and AOV $\theta_i = \pi/3$.

Results. The simulation results are presented in Fig. 5, where we observe a trade-off of ANACONDA between centralization and decentralization, where increasing α_i or c_i generally improves coverage after convergence but at the cost of more decision rounds. Both parameters follow the principle of diminishing marginal returns due to the submodularity of VoC: while larger α_i and c_i values enhance the agents’ information access, the gains eventually become incremental. Furthermore, larger c_i values significantly increase the number of decision rounds required to converge, meaning that highly centralized configurations may underperform compared to the benchmarks in shorter time horizons. Moreover, ANACONDA consistently achieves improved asymptotic coverage over these benchmarks as long as α_i or c_i are not too small, suggesting that intermediate parameter values, such as $c_i = 16$, offer the most effective balance between real-time convergence and long-term performance. We conjecture that ANACONDA’s improved performance arises from richer information mixing enabled by the time-varying communication neighborhoods, as opposed to the benchmarks’ sequential information passing.

C. Comparison with Delays: Coverage vs. Actual Time

We compare ANACONDA with DFS-SG and DFS-BSG in 20 MC trials under three delay configurations $(\tau_f, \tau_c) \in \{(.01s, .03s), (.03s, .03s), (.09s, .03s)\}$, capturing different computation and communication capabilities. Each trial is carried out over a fixed 300s time horizon.

Setup. The setup is identical to that in Fig. 5(b), with the communication range $c_i = 16$ for all cameras $i \in \mathcal{N}$.

Results. The simulation results are presented in Fig. 6 and Table II where we observe the following for ANACONDA: {ANACONDA demonstrates a better performance than DFS-BSG and can outperform DFS-SG after convergence. The reason is that ANACONDA decides actions much faster than DFS-BSG in large networks, which means much more decision rounds in a fixed time horizon.

TABLE II: Comparison of average coverage performance (%) within 300s across three scenarios with different delay configurations (Fig. 6). The highest value in each scenario is highlighted in **bold**.

Algorithm	Coverage (%)		
	$\tau_f = .01s, \tau_c = .03s$	$\tau_f = .03s, \tau_c = .03s$	$\tau_f = .09s, \tau_c = .03s$
DFS-BSG	42.19 \pm 1.83	41.96 \pm 1.98	42.30 \pm 2.20
ANACONDA-0N	47.33 \pm 1.84	46.52 \pm 1.92	46.78 \pm 1.77
ANACONDA-1N	58.27 \pm 1.22	56.13 \pm 1.77	52.17 \pm 1.68
ANACONDA-2N	58.75 \pm 1.18	56.75 \pm 1.28	51.68 \pm 1.90
ANACONDA-3N	59.05 \pm 0.89	57.10 \pm 1.04	51.73 \pm 0.91
ANACONDA-4N	59.08 \pm 0.82	56.20 \pm 1.57	50.12 \pm 0.93
ANACONDA-5N	59.12 \pm 1.01	55.72 \pm 1.32	49.99 \pm 1.73

Increasing the neighborhood size α_i presents a trade-off for ANACONDA: although larger neighborhoods theoretically offer higher asymptotic coverage, they also increase computation time per round, resulting in fewer decision cycles within a fixed time horizon. For example, in Fig. 6(a)–(c), the best-performing communication neighborhood sizes within the 300s window are $\alpha_i = 5, 3$, and 1, respectively, rather than always 5 (Table II). This “no free neighbor” dynamic, characterized by a cubic growth in convergence time relative to α_i , means that smaller neighborhood sizes can yield better performance in a fixed horizon.

D. Scalability

We finally compare the real-time coverage performance of ANACONDA-5N and DFS-BSG over 20 MC trials as the network size scales across five scenarios with varying numbers of cameras and map sizes. Each trial is executed over a fixed time horizon of 300s with $(\tau_f, \tau_c) = (0.01s, 0.01s)$.

Setup. The five scenarios contain $\{10, 20, 30, 40, 50\}$ cameras deployed in maps of sizes $\{23^2, 32^2, 39^2, 45^2, 50^2\}$, respectively. These configurations maintain an approximately constant camera density, with each camera covering roughly 50 square units on average. Across all scenarios, the communication range is fixed at $c_i = 16$ for all cameras $i \in \mathcal{N}$.

Results. ANACONDA scales despite imperfect communication; DFS-BSG does not. Per Fig. 7, when the network size increases from 10 to 50 agents, ANACONDA consistently executes 2142 rounds, owing to its fixed per-round computation and communication load (Proposition 5), and the convergence time grows from 100s to 200s, which is a sublinear growth in $|\mathcal{N}|$. In contrast, the number of rounds completed by DFS-BSG declines from 493 to just 15, because each round requires sequential communication across the entire network.

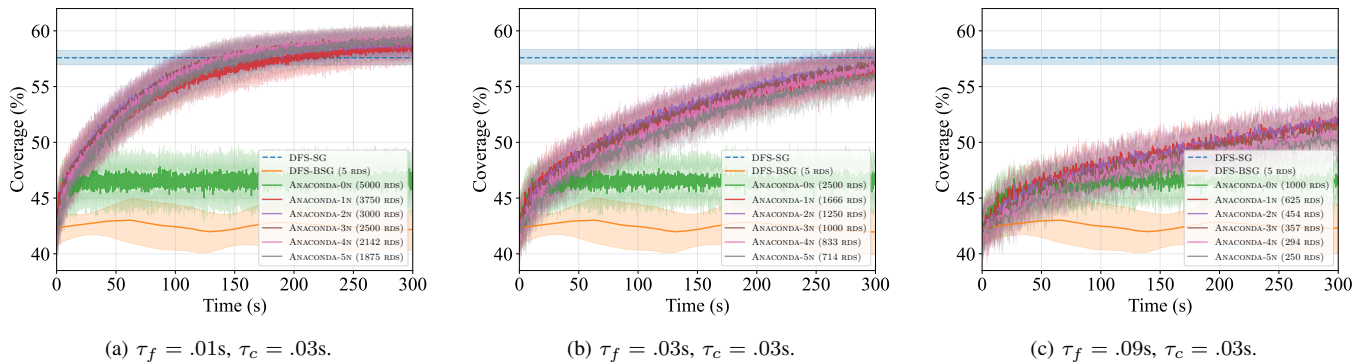


Fig. 6: **Comparison of ANACONDA vs. DFS-SG vs. DFS-BSG for real-time coverage performance under computation and communication delays.** Cameras select their FOV directions using ANACONDA with maximum communication neighborhood sizes in $\{0, \dots, 5\}$, or using DFS-SG or DFS-BSG. From (a) to (b) to (c), the time τ_f for one function evaluation increases relative to the delay τ_c for transmitting one action through a communication link, with the ratio τ_f/τ_c taking values $1/3$, 1 , and 3 . DFS-SG is executed for a single decision round, whereas the other algorithms are run for a fixed duration of 300 seconds. Under different delay configurations, the algorithms complete different numbers of decision rounds within this time window. Results are averaged over 20 Monte Carlo trials.

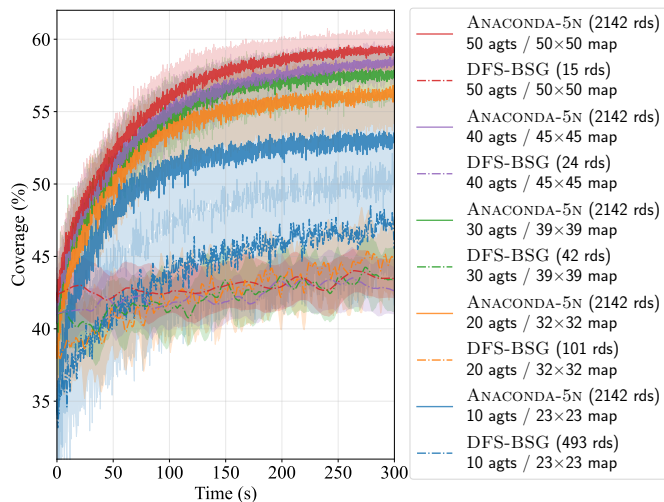


Fig. 7: **Comparison of ANACONDA-5N vs. DFS-BSG in real-time coverage performance with scaling network.** Cameras select their FOV directions using ANACONDA-5N or DFS-BSG, across five scenarios with different network and map sizes. To keep the camera density constant, the map size scales linearly from 23×23 to 50×50 as the network size ranges from 10 to 50. Results are averaged over 20 Monte Carlo trials, each with a fixed 300s time window under delays $(\tau_f, \tau_c) = (.01s, .01s)$.

VIII. CONCLUSION

We presented ANACONDA, a scalable framework for distributed submodular coordination in multi-agent systems operating in unknown environments under realistic communication constraints. ANACONDA achieves scalability while maintaining near-optimal action coordination by intelligently limiting communication, regardless of global connectivity. We introduced a novel metric, VoC, that quantifies the benefit of information access for coordination. By optimizing VoC, the framework enables intelligent information limitation through communication neighborhood design. The suboptimality guarantees showed that ANACONDA’s coordination performance improves with the sum of all agents’ VoC, and is anytime non-trivial even prior to convergence. Extensive simulations in multi-camera area monitoring against state-of-the-art benchmarks supported the theoretical analysis and illustrated ANACONDA’s benefit in coordination performance, neighborhood

design, and scalability, together with a fundamental trade-off between coordination optimality and convergence speed under realistic communication latency.

Future work. While ANACONDA demonstrates improvement in decision time compared to benchmarks for unknown environments, for mobile-robot applications, we will work to accelerate it to $O(|\mathcal{N}|)$ decision time, leveraging the tools in [52]. Moreover, while the coordination neighborhood \mathcal{M}_i is currently considered static, it can be dynamic for mobile robots. To this end, we will also handle dynamic coordination neighborhoods, *i.e.*, $\mathcal{M}_{i,t}$, with guaranteed performances.

REFERENCES

- [1] Z. Xu, X. Lin, and V. Tzoumas, “Bandit submodular maximization for multi-robot coordination in unpredictable and partially observable environments,” in *Robotics: Science and Systems (RSS)*, 2023.
- [2] N. Atanasov, J. Le Ny, K. Daniilidis, and G. J. Pappas, “Decentralized active information acquisition: Theory and application to multi-robot SLAM,” in *IEEE Inter. Conf. Rob. Auto. (ICRA)*, 2015, pp. 4775–4782.
- [3] M. Corah and N. Michael, “Distributed submodular maximization on partition matroids for planning on large sensor networks,” in *IEEE Conference on Decision and Control (CDC)*, 2018, pp. 6792–6799.
- [4] A. Jadbabaie, J. Lin, and A. Morse, “Coordination of groups of mobile autonomous agents using nearest neighbor rules,” *IEEE Transactions on Automatic Control (TAC)*, vol. 48, no. 6, pp. 988–1001, 2003.
- [5] A. Nedic and A. Ozdaglar, “Distributed subgradient methods for multi-agent optimization,” *IEEE Transactions on Automatic Control (TAC)*, vol. 54, no. 1, pp. 48–61, 2009.
- [6] Digi International. (2025) XBee 3 Zigbee 3 RF Module Specifications. Accessed: Dec. 2025. [Online]. Available: <https://www.digi.com/products/embedded-systems/digi-xbee/rf-modules/2-4-ghz-rf-modules/xbee3-zigbee-3#specifications>
- [7] Silvus Technologies. (2025) StreamCaster Lite 5200 (SL5200) MANET Radio Specifications. Accessed: Dec. 2025. [Online]. Available: <https://silvustechtechnologies.com/products/streamcaster-lite-5200/>
- [8] T. F. Internet. (2025) Wifi 6 vs wifi 6e: Unlocking faster, more reliable connectivity. Accessed: Dec. 2025. [Online]. Available: <https://tachus.com/wifi-6-vs-wifi-6e/>
- [9] Y. Kantaros, M. Guo, and M. M. Zavlanos, “Temporal logic task planning and intermittent connectivity control of mobile robot networks,” *IEEE Transactions on Automatic Control (TAC)*, vol. 64, no. 10, pp. 4105–4120, 2019.
- [10] T. Lattimore and C. Szepesvári, *Bandit Algorithms*. Cambridge University Press, 2020.
- [11] A. Krause, A. Singh, and C. Guestrin, “Near-optimal sensor placements in gaussian processes: Theory, efficient algorithms and empirical studies,” *Jour. Mach. Learn. Res. (JMLR)*, vol. 9, pp. 235–284, 2008.
- [12] A. Singh, A. Krause, C. Guestrin, and W. J. Kaiser, “Efficient informative sensing using multiple robots,” *Journal of Artificial Intelligence Research (JAIR)*, vol. 34, pp. 707–755, 2009.

- [13] P. Tokekar, V. Isler, and A. Franchi, “Multi-target visual tracking with aerial robots,” in *IEEE/RSJ International Conference on Intelligent Robots and Systems (IROS)*, 2014, pp. 3067–3072.
- [14] B. Ghahsifard and S. L. Smith, “Distributed submodular maximization with limited information,” *IEEE Transactions on Control of Network Systems (TCNS)*, vol. 5, no. 4, pp. 1635–1645, 2017.
- [15] J. R. Marden, “The role of information in distributed resource allocation,” *IEEE Transactions on Control of Network Systems (TCNS)*, vol. 4, no. 3, pp. 654–664, 2017.
- [16] D. Grimsman, M. S. Ali, J. P. Hespanha, and J. R. Marden, “The impact of information in distributed submodular maximization,” *IEEE Trans. Ctrl. Netw. Sys. (TCNS)*, vol. 6, no. 4, pp. 1334–1343, 2019.
- [17] B. Schlotfeldt, V. Tzoumas, and G. J. Pappas, “Resilient active information acquisition with teams of robots,” *IEEE Transactions on Robotics (TRO)*, vol. 38, no. 1, pp. 244–261, 2021.
- [18] B. Du, K. Qian, C. Claudel, and D. Sun, “Jacobi-style iteration for distributed submodular maximization,” *IEEE Transactions on Automatic Control (TAC)*, vol. 67, no. 9, pp. 4687–4702, 2022.
- [19] N. Reza zadeh and S. S. Kia, “Distributed strategy selection: A submodular set function maximization approach,” *Automatica*, vol. 153, p. 111000, 2023.
- [20] A. Robey, A. Adibi, B. Schlotfeldt, H. Hassani, and G. J. Pappas, “Optimal algorithms for submodular maximization with distributed constraints,” in *Learn. for Dyn. & Cont. (LADC)*, 2021, pp. 150–162.
- [21] Z. Xu, S. S. Garimella, and V. Tzoumas, “Communication- and computation-efficient distributed submodular optimization in robot mesh networks,” *IEEE Transactions on Robotics (TRO)*, 2025.
- [22] M. L. Fisher, G. L. Nemhauser, and L. A. Wolsey, “An analysis of approximations for maximizing submodular set functions–II,” in *Polyhedral combinatorics*, 1978, pp. 73–87.
- [23] U. Feige, “A threshold of $\ln(n)$ for approximating set cover,” *Journal of the ACM (JACM)*, vol. 45, no. 4, pp. 634–652, 1998.
- [24] J. Liu, L. Zhou, P. Tokekar, and R. K. Williams, “Distributed resilient submodular action selection in adversarial environments,” *IEEE Robotics and Automation Letters (RAL)*, vol. 6, no. 3, pp. 5832–5839, 2021.
- [25] R. Konda, D. Grimsman, and J. R. Marden, “Execution order matters in greedy algorithms with limited information,” in *American Control Conference (ACC)*, 2022, pp. 1305–1310.
- [26] A. Krause and D. Golovin, “Submodular function maximization,” *Tractability: Practical Approaches to Hard Problems*, vol. 3, 2012.
- [27] M. Streeter and D. Golovin, “An online algorithm for maximizing submodular functions,” *Adv. Neu. Inf. Proc. Sys.*, vol. 21, 2008.
- [28] M. Streeter, D. Golovin, and A. Krause, “Online learning of assignments,” *Adv. Neu. Info. Proc. Sys. (NeurIPS)*, vol. 22, 2009.
- [29] D. Suehiro, K. Hatano, S. Kijima, E. Takimoto, and K. Nagano, “Online prediction under submodular constraints,” in *International Conf. on Algorithmic Learning Theory (ALT)*, 2012, pp. 260–274.
- [30] D. Golovin, A. Krause, and M. Streeter, “Online submodular maximization under a matroid constraint with application to learning assignments,” *arXiv preprint:1407.1082*, 2014.
- [31] L. Chen, H. Hassani, and A. Karbasi, “Online continuous submodular maximization,” in *International Conference on Artificial Intelligence and Statistics (AISTATS)*. PMLR, 2018, pp. 1896–1905.
- [32] M. Zhang, L. Chen, H. Hassani, and A. Karbasi, “Online continuous submodular maximization: From full-information to bandit feedback,” *Adv. Neu. Info. Proc. Sys. (NeurIPS)*, vol. 32, 2019.
- [33] Z. Xu, H. Zhou, and V. Tzoumas, “Online submodular coordination with bounded tracking regret: Theory, algorithm, and applications to multi-robot coordination,” *IEEE Robotics and Automation Letters (RAL)*, vol. 8, no. 4, pp. 2261–2268, 2023.
- [34] G. Calinescu, C. Chekuri, M. Pál, and J. Vondrák, “Maximizing a monotone submodular function subject to a matroid constraint,” *SIAM Journal on Computing*, vol. 40, no. 6, pp. 1740–1766, 2011.
- [35] A. Mokhtari, H. Hassani, and A. Karbasi, “Decentralized submodular maximization: Bridging discrete and continuous settings,” in *International Conference on Machine Learning (ICML)*, 2018, pp. 3616–3625.
- [36] L. Chen, M. Zhang, H. Hassani, and A. Karbasi, “Black box submodular maximization: Discrete and continuous settings,” in *Inter. Conf. Arti. Intel. Stats. (AISTATS)*. PMLR, 2020, pp. 1058–1070.
- [37] Q. Zhang, Z. Wan, Y. Yang, L. Shen, and D. Tao, “Near-optimal online learning for multi-agent submodular coordination: Tight approximation and communication efficiency,” *arXiv preprint:2502.05028*, 2025.
- [38] A. I. Rikos, W. Jiang, T. Charalambous, and K. H. Johansson, “Asynchronous distributed optimization via admm with efficient communication,” in *IEEE Conference on Decision and Control (CDC)*, 2023, pp. 7002–7008.
- [39] J. Hu, K. H. Johansson, and A. I. Rikos, “Distributed quantized average consensus in open multi-agent systems with dynamic communication links,” *arXiv preprint:2508.05895*, 2025.
- [40] M. Bianchi and S. Grammatico, “The END: Estimation network design for games under partial-decision information,” *IEEE Transactions on Control of Network Systems (TCNS)*, vol. 11, no. 4, pp. 2200–2212, 2024.
- [41] B. Zhou, H. Xu, and S. Shen, “Racer: Rapid collaborative exploration with a decentralized multi-uav system,” *IEEE Transactions on Robotics (TRO)*, vol. 39, no. 3, pp. 1816–1835, 2023.
- [42] X. Liu, J. Lei, A. Prabhu, Y. Tao, I. Spasojevic, P. Chaudhari, N. Atanasov, and V. Kumar, “SlideSLAM: Sparse, lightweight, decentralized metric-semantic slam for multirobot navigation,” *IEEE Transactions on Robotics (TRO)*, vol. 41, pp. 6529–6548, 2025.
- [43] Z. Xu and V. Tzoumas, “Performance-aware self-configurable multi-agent networks: A distributed submodular approach for simultaneous coordination and network design,” in *IEEE Conference on Decision and Control (CDC)*, 2024, pp. 5393–5400.
- [44] Y. Crama, P. L. Hammer, and R. Holzman, “A characterization of a cone of pseudo-boolean functions via supermodularity-type inequalities,” in *Quantitative Methoden in den Wirtschaftswissenschaften*. Springer, 1989, pp. 53–55.
- [45] S. Foldes and P. L. Hammer, “Submodularity, supermodularity, and higher-order monotonicities of pseudo-boolean functions,” *Mathematics of Operations Research*, vol. 30, no. 2, pp. 453–461, 2005.
- [46] P. Auer, N. Cesa-Bianchi, Y. Freund, and R. E. Schapire, “The non-stochastic multiarmed bandit problem,” *SIAM Journal on Computing*, vol. 32, no. 1, pp. 48–77, 2002.
- [47] G. Neu, “Explore no more: Improved high-probability regret bounds for non-stochastic bandits,” *Adv. Neu. Info. Proc. Sys.*, vol. 28, 2015.
- [48] Y. Seldin and A. Slivkins, “One practical algorithm for both stochastic and adversarial bandits,” in *International Conference on Machine Learning (ICML)*, 2014, pp. 1287–1295.
- [49] J. Zimmert and Y. Seldin, “Tsallis-INF: An optimal algorithm for stochastic and adversarial bandits,” *Journal of Machine Learning Research (JMLR)*, vol. 22, no. 28, pp. 1–49, 2021.
- [50] M. Conforti and G. Cornuéjols, “Submodular set functions, matroids and the greedy algorithm: Tight worst-case bounds and some generalizations of the rado-edmonds theorem,” *Discrete Applied Mathematics*, vol. 7, no. 3, pp. 251–274, 1984.
- [51] T. Matsuoka, S. Ito, and N. Ohsaka, “Tracking regret bounds for online submodular optimization,” in *International Conference on Artificial Intelligence and Statistics (AISTATS)*. PMLR, 2021, pp. 3421–3429.
- [52] A. Rakhlin and K. Sridharan, “Online learning with predictable sequences,” in *Conference on Learning Theory (COLT)*, 2013, pp. 993–1019.
- [53] V. Tzoumas, K. Gatsis, A. Jadbabaie, and G. J. Pappas, “Resilient monotone submodular function maximization,” in *IEEE Conference on Decision and Control (CDC)*, 2017, pp. 1362–1367.

APPENDIX A

SUBOPTIMALITY GUARANTEES OF ANACONDA

We will first prove Lemmas 1 to 3, then Proposition 1 and Theorems 1 to 3.

Proof of Lemma 1. Consider $\text{VoC}_{f,t}(a; \mathcal{J}) = f(a) - f(a | \{a_j\}_{j \in \mathcal{J}})$, where $\mathcal{J} \subseteq \mathcal{M}_i \subseteq \mathcal{N} \setminus \{i\}$, $a \in \mathcal{V}_i$ is fixed, and $f: 2^{\mathcal{V}_N} \mapsto \mathbb{R}$ is non-decreasing and 2nd-order submodular. Also, with a slight abuse of notation, denote $f(a | \{a_j\}_{j \in \mathcal{J}})$ by $f(a | \mathcal{J})$.

To prove the monotonicity of $\text{VoC}_{f,t}(a; \cdot)$, consider $\mathcal{A}_1, \mathcal{A}_2 \subseteq \mathcal{M}_i$ that are disjoint. Then, $\text{VoC}_{f,t}(a; \mathcal{A}_1 \cup \mathcal{A}_2) - \text{VoC}_{f,t}(a; \mathcal{A}_1) = -f(a | \mathcal{A}_1 \cup \mathcal{A}_2) + f(a | \mathcal{A}_1) \geq 0$ since f is submodular. Thus, $\text{VoC}_{f,t}(a; \cdot)$ is non-decreasing.

To prove the submodularity of $\text{VoC}_{f,t}(a; \cdot)$, consider

$\mathcal{A}, \mathcal{B}_1, \mathcal{B}_2 \subseteq \mathcal{V}$, where \mathcal{B}_1 and \mathcal{B}_2 are disjoint, then:

$$\begin{aligned} & \text{VoC}_{f,t}(a; \mathcal{A} | \mathcal{B}_1) - \text{VoC}_{f,t}(a; \mathcal{A} | \mathcal{B}_1 \cup \mathcal{B}_2) \\ &= \text{VoC}_{f,t}(a; \mathcal{A} \cup \mathcal{B}_1) - \text{VoC}_{f,t}(a; \mathcal{B}_1) \\ &\quad - \text{VoC}_{f,t}(a; \mathcal{A} \cup \mathcal{B}_1 \cup \mathcal{B}_2) + \text{VoC}_{f,t}(a; \mathcal{B}_1 \cup \mathcal{B}_2) \\ &= -f(a | \mathcal{A} \cup \mathcal{B}_1) + f(a | \mathcal{B}_1) \\ &\quad + f(a | \mathcal{A} \cup \mathcal{B}_1 \cup \mathcal{B}_2) - f(a | \mathcal{B}_1 \cup \mathcal{B}_2) \geq 0, \end{aligned} \quad (23)$$

where the inequality holds since f is 2nd-order submodular (Definition 2). Therefore, $\text{VoC}_{f,t}(a; \cdot)$ is submodular. \square

Proof of Lemma 2. According to [46, Theorem 3.1], we have $\text{A-Reg}_T(\{a_{i,t}\}_{t \in [T]}) \leq \sqrt{2T} |\mathcal{V}_i| \log |\mathcal{V}_i|$. \square

Proof of Lemma 3. Given Definition 6, we have

$$\begin{aligned} & \text{N-Reg}_{\{a_{i,t}\}_{t \in [T]}}^{\rho(\kappa_{I,i}, \alpha_i)}(\{\mathcal{N}_{i,t}\}_{t \in [T]}) \\ &= \rho(\kappa_{I,i}, \alpha_i) \max_{\mathcal{N}_{i,t} \subseteq \mathcal{M}_i, |\mathcal{N}_{i,t}| \leq \alpha_i} \sum_{t=1}^T \text{VoC}_{f,t}(a_{i,t}; \mathcal{N}_{i,t}) \\ &\quad - \sum_{t=1}^T \text{VoC}_{f,t}(a_{i,t}; \mathcal{N}_{i,t}) \\ &\leq \rho(\kappa_{I,i}, \alpha_i) \sum_{t=1}^T \left(-\alpha_i r_{j_{k,t},t} + \sum_{k=1}^{\alpha_i} r_{j_{k,t},t}^{\text{OPT}} \right) \end{aligned} \quad (24)$$

$$= \rho(\kappa_{I,i}, \alpha_i) \sum_{k=1}^{\alpha_i} \mathbb{E} \left[\sum_{t=1}^T \left(r_{j_{k,t},t}^{\text{OPT}} - r_{j_{k,t},t}^{\top} q_{k,t} \right) \right] \quad (25)$$

$$\leq \tilde{O} \left(\alpha_i \sqrt{|\mathcal{M}_i| T} \right), \quad (26)$$

where eq. (24) follows from [51, Theorem 3], eq. (25) follows from the linearity of expectation, and eq. (26) follows by applying [46, Theorem 3.1]. \square

Proofs of Proposition 1 and Theorem 1. We have:

$$\begin{aligned} & \sum_{t=1}^T f(\mathcal{A}^{\text{OPT}}) \\ &= \sum_{t=1}^T f(\mathcal{A}^{\text{OPT}} \cup \mathcal{A}_t) - \sum_{t=1}^T \sum_{i \in \mathcal{N}} f(a_{i,t} | \mathcal{A}^{\text{OPT}} \cup \{a_{j,t}\}_{j \in [i-1]}) \end{aligned} \quad (27)$$

$$\begin{aligned} & \leq \sum_{t=1}^T f(\mathcal{A}_t) + \sum_{t=1}^T \sum_{i \in \mathcal{N}} f(a_i^{\text{OPT}} | \mathcal{A}_t) \\ &\quad - (1 - \kappa_f) \sum_{t=1}^T \sum_{i \in \mathcal{N}} f(a_{i,t} | \{a_{j,t}\}_{j \in \mathcal{N}_{i,t}}) \end{aligned} \quad (28)$$

$$\begin{aligned} & \leq \sum_{t=1}^T f(\mathcal{A}_t) + \kappa_f \sum_{t=1}^T \sum_{i \in \mathcal{N}} f(a_{i,t} | \{a_{j,t}\}_{j \in \mathcal{N}_{i,t}}) \\ &\quad + \sum_{i \in \mathcal{N}} \sum_{t=1}^T [f(a_i^{\text{OPT}} | \{a_{j,t}\}_{j \in \mathcal{N}_{i,t}}) - f(a_{i,t} | \{a_{j,t}\}_{j \in \mathcal{N}_{i,t}})] \end{aligned} \quad (29)$$

$$\begin{aligned} & \leq \sum_{t=1}^T f(\mathcal{A}_t) + \kappa_f \sum_{t=1}^T \sum_{i \in \mathcal{N}} f(a_{i,t} | \{a_{j,t}\}_{j \in \mathcal{N}_{i,t}}) \\ &\quad + \sum_{i \in \mathcal{N}} \text{A-Reg}_T(\{a_{i,t}\}_{t \in [T]}) \end{aligned} \quad (30)$$

$$\begin{aligned} &= \sum_{t=1}^T f(\mathcal{A}_t) - \kappa_f \sum_{i \in \mathcal{N}} \sum_{t=1}^T \text{VoC}_{f,t}(a_{i,t}; \mathcal{N}_{i,t}) \\ &\quad + \kappa_f \sum_{t=1}^T \sum_{i \in \mathcal{N}} f(a_{i,t}) + \sum_{i \in \mathcal{N}} \text{A-Reg}_T(\{a_{i,t}\}_{t \in [T]}) \end{aligned} \quad (31)$$

$$\begin{aligned} & \leq \sum_{t=1}^T f(\mathcal{A}_t) + \frac{\kappa_f}{1 - \kappa_f} \sum_{t=1}^T \sum_{i \in \mathcal{N}} f(a_{i,t} | \{a_{j,t}\}_{j \in [i-1]}) \\ &\quad - \kappa_f \rho(\kappa_I, \bar{\alpha}) \sum_{i \in \mathcal{N}} \sum_{t=1}^T \text{VoC}_{f,t}(a_{i,t}; \mathcal{N}_i^*(\{a_{i,t}\}_{t \in [T]}; \alpha_i, \mathcal{M}_i)) \\ &\quad + \kappa_f \sum_{i \in \mathcal{N}} \text{N-Reg}_{\{a_{i,t}\}_{t \in [T]}}^{\rho(\kappa_I, \bar{\alpha})}(\{\mathcal{N}_{i,t}\}_{t \in [T]}) \\ &\quad + \sum_{i \in \mathcal{N}} \text{A-Reg}_T(\{a_{i,t}\}_{t \in [T]}) \end{aligned} \quad (32)$$

$$\begin{aligned} & \leq \sum_{t=1}^T f(\mathcal{A}_t) + \frac{\kappa_f}{1 - \kappa_f} \sum_{t=1}^T f(\mathcal{A}_t) \\ &\quad - \kappa_f \rho(\kappa_I, \bar{\alpha}) \sum_{i \in \mathcal{N}} \sum_{t=1}^T \text{VoC}_{f,t}(a_{i,t}; \mathcal{N}_i^*(\{a_{i,t}\}_{t \in [T]}; \alpha_i, \mathcal{M}_i)) \\ &\quad + \tilde{O} \left(|\mathcal{N}| \sqrt{|\bar{\mathcal{V}}| T} \right) + \tilde{O} \left(|\mathcal{N}| \bar{\alpha} \sqrt{|\bar{\mathcal{M}}| T} \right), \end{aligned} \quad (33)$$

where eq. (27) holds by telescoping the sum, eq. (28) holds since f is submodular and since $1 - \kappa_f \leq \frac{f(a_{i,t} | \{a_{j,t}\}_{j \in \mathcal{N} \setminus \{i\}})}{f(a_{i,t})} \leq \frac{f(a_{i,t} | \mathcal{A}^{\text{OPT}} \cup \{a_{j,t}\}_{j \in [i-1]})}{f(a_{i,t} | \{a_{j,t}\}_{j \in \mathcal{N}_{i,t}})}$ per Definition 4, eq. (29) holds from submodularity, eq. (30) holds from Definition 5; eq. (31) holds from Definition 3, eq. (32) holds from Definition 6, and eq. (33) holds from Lemmas 2 and 3.

Simplifying eq. (33), we have

$$\begin{aligned} f(\mathcal{A}^{\text{OPT}}) &= \frac{1}{T} \sum_{t=1}^T f(\mathcal{A}^{\text{OPT}}) \\ &\leq \frac{1}{1 - \kappa_f} \mathbb{E} [f(\mathcal{A}_t)] \\ &\quad - \kappa_f \rho(\kappa_I, \bar{\alpha}) \sum_{i \in \mathcal{N}} \sum_{t=1}^T \text{VoC}_{f,t}(a_{i,t}; \mathcal{N}_i^*(\{a_{i,t}\}_{t \in [T]}; \alpha_i, \mathcal{M}_i)) \\ &\quad + \tilde{O} \left(|\mathcal{N}| \sqrt{(\bar{\alpha}^2 |\bar{\mathcal{M}}| + |\bar{\mathcal{V}}|) / T} \right). \end{aligned} \quad (34)$$

Therefore,

$$\begin{aligned} \mathbb{E} [f(\mathcal{A}_t)] &\geq (1 - \kappa_f) f(\mathcal{A}^{\text{OPT}}) \\ &\quad + \kappa_f (1 - \kappa_f) \rho(\kappa_I, \bar{\alpha}) \\ &\quad \times \sum_{i \in \mathcal{N}} \mathbb{E} [\text{VoC}_{f,t}(a_{i,t}; \mathcal{N}_i^*(\{a_{i,t}\}_{t \in [T]}; \alpha_i, \mathcal{M}_i))] \\ &\quad - \tilde{O} \left(|\mathcal{N}| \sqrt{(\bar{\alpha}^2 |\bar{\mathcal{M}}| + |\bar{\mathcal{V}}|) / T} \right), \end{aligned} \quad (35)$$

and, thus, eq. (14) is proved.

To prove eq. (15), where $\mathcal{N}_{i,t} \equiv \mathcal{M}_i = \mathcal{N} \setminus \{i\}$:

$$\mathbb{E}[f(\mathcal{A}_t)] \geq f(\mathcal{A}^{\text{OPT}}) - \kappa_f \sum_{i \in \mathcal{N}} \mathbb{E}[f(a_{i,t} | \mathcal{A}_t \setminus \{a_{i,t}\})] - \tilde{O}\left(|\mathcal{N}| \sqrt{|\bar{\mathcal{V}}|/T}\right) \quad (36)$$

$$\geq f(\mathcal{A}^{\text{OPT}}) - \kappa_f \mathbb{E}[f(\mathcal{A}_t)] - \tilde{O}\left(|\mathcal{N}| \sqrt{|\bar{\mathcal{V}}|/T}\right), \quad (37)$$

where eq. (36) holds from eq. (30), and eq. (37) holds from [53, Eq. (15)]. Thereby,

$$\mathbb{E}[f(\mathcal{A}_t)] \geq \frac{1}{1 + \kappa_f} f(\mathcal{A}^{\text{OPT}}) - \tilde{O}\left(|\mathcal{N}| \sqrt{|\bar{\mathcal{V}}|/T}\right). \quad (38)$$

To prove eq. (16), where $\mathcal{N}_{i,t} \equiv \emptyset$, per eq. (30),

$$\begin{aligned} \mathbb{E}[f(\mathcal{A}_t)] &\geq f(\mathcal{A}^{\text{OPT}}) - \kappa_f \sum_{i \in \mathcal{N}} \mathbb{E}[f(a_{i,t})] - \tilde{O}\left(|\mathcal{N}| \sqrt{|\bar{\mathcal{V}}|/T}\right) \\ &\geq f(\mathcal{A}^{\text{OPT}}) - \frac{\kappa_f}{1 - \kappa_f} \mathbb{E}[f(\mathcal{A}_t)] - \tilde{O}\left(|\mathcal{N}| \sqrt{|\bar{\mathcal{V}}|/T}\right). \end{aligned} \quad (39)$$

Therefore,

$$\mathbb{E}[f(\mathcal{A}_t)] \geq (1 - \kappa_f) f(\mathcal{A}^{\text{OPT}}) - \tilde{O}\left(|\mathcal{N}| \sqrt{|\bar{\mathcal{V}}|/T}\right). \quad (40)$$

□

Proofs of Theorems 2 and 3. Dividing both sides of eq. (30) by $\sum_{t=1}^T f(\mathcal{A}_t)$, we have

$$\frac{\sum_{t=1}^T f(\mathcal{A}^{\text{OPT}})}{\sum_{t=1}^T f(\mathcal{A}_t)} \leq 1 + \kappa_f \frac{\sum_{t=1}^T \sum_{i \in \mathcal{N}} f(a_{i,t} | \{a_{j,t}\}_{j \in \mathcal{N}_{i,t}})}{\sum_{t=1}^T f(\mathcal{A}_t)} + \tilde{O}\left(|\mathcal{N}| \sqrt{|\bar{\mathcal{V}}|/T}\right) \quad (41)$$

$$= 1 + \beta \kappa_f + \tilde{O}\left(|\mathcal{N}| \sqrt{|\bar{\mathcal{V}}|/T}\right), \quad (42)$$

and thus Theorem 2 holds. In particular, if at any time t there exists an agent ordering such that $[i-1] \subseteq \mathcal{N}_{i,t}, \forall i$, then

$$\begin{aligned} 0 \leq \beta &= \frac{\sum_{t=1}^T \sum_{i \in \mathcal{N}} f(a_{i,t} | \{a_{j,t}\}_{j \in \mathcal{N}_{i,t}})}{\sum_{t=1}^T f(\mathcal{A}_t)} \\ &\leq \frac{\sum_{t=1}^T \sum_{i \in \mathcal{N}} f(a_{i,t} | \{a_{j,t}\}_{j \in [i-1]})}{\sum_{t=1}^T f(\mathcal{A}_t)} = 1 \end{aligned} \quad (43)$$

holds due to submodularity. Finally, combining eqs. (16) and (19), Theorem 3 holds. □

APPENDIX B DECISION TIME OF ANACONDA

We will first present and prove the following propositions and then prove Theorem 4.

Proposition 2 (Convergence Rate). ANACONDA's convergence error takes T iterations to be within ϵ where

- If NEISEL is not involved, i.e., $\forall i, \alpha_i = 0$ or $\alpha_i \geq |\mathcal{M}_i|$,

$$T \geq |\bar{\mathcal{V}}| |\mathcal{N}|^2 / \epsilon, \quad (44)$$

- If NEISEL is involved, i.e., $\exists i \in \mathcal{N}, 0 < \alpha_i < |\mathcal{M}_i|$,

$$T \geq (\bar{\alpha}^2 |\bar{\mathcal{M}}| + |\bar{\mathcal{V}}|) |\mathcal{N}|^2 / \epsilon. \quad (45)$$

Proof: Proposition 2 holds from Lemmas 2 and 3. □

Proposition 3 (Computational Complexity). At each $t \in [T]$, ANACONDA requires each agent i to execute $2\alpha_i + 3$ evaluations of f and $O(|\mathcal{V}_i| + \alpha_i |\mathcal{M}_i|)$ additions/multiplications.

Proof: At each $t \in [T]$, ACTSEL requires 2 function evaluations (Algorithm 2's line 7), along with $O(|\mathcal{V}_i|)$ additions and multiplications (Algorithm 2's lines 4 and 8). Also, NEISEL requires $2\alpha_i + 1$ function evaluations (Algorithm 3's line 9), along with $O(\alpha_i |\mathcal{M}_i|)$ additions and multiplications (Algorithm 3's lines 6 and 9-11). □

Proposition 4 (Communication Complexity). At each $t \in [T]$, ANACONDA requires one communication round where each agent i only transmits its own action to its out-neighbors.

Proof: At each $t \in [T]$, ANACONDA requires one (multi-channel) communication round where each agent i shares $a_{i,t}$ with and simultaneously receives $\{a_{j,t}\}_{j \in \mathcal{N}_{i,t}}$ from $\mathcal{N}_{i,t}$ (Algorithm 1's line 5).

Proposition 5 (Per-Round Decision Time). One round of ANACONDA takes $\tau_f (2\alpha_i + 3) + \tau_c$ time to complete.

Proof: Proposition 5 holds because of Propositions 3 and 4, ignoring the time for additions and multiplications. □

Finally, we prove Theorem 4:

Proof of Theorem 4. Theorem 4 holds because of Propositions 2 and 5. □

APPENDIX C WORST-CASE DECISION TIME OF SEQUENTIAL COMMUNICATION IN DIRECTED NETWORKS

We prove that DFS-SG has a $O(\tau_c |\mathcal{N}|^3)$ worst-case communication time on a strongly connected directed graph. The proof extends [25, Section III-D] by taking also the size of each inter-agent communication message into consideration since the larger the size the more time it will take for the message to be transmitted. We use the notation:

- $\mathcal{G}_{dir} = \{\mathcal{N}, \mathcal{E}_{dir}\}$ is a strongly connected directed graph;
- $\pi: \{1, \dots, |\mathcal{N}|\} \mapsto \{1, \dots, |\mathcal{N}|\}$ denotes the order of action selection for agent $i \in \mathcal{N}$ given by the DFS approach in [25];
- $d(i, j)$ denotes the length of the shortest path from agent i to j on \mathcal{G}_{dir} .

Suppose $p = (v_1, \dots, v_l)$ is the longest path of \mathcal{G}_{dir} , where $l = |p|$. If $l = |\mathcal{N}|$, then p is a spanning walk on \mathcal{G}_{dir} with $\pi(i) = i, \forall i = \{1, \dots, |\mathcal{N}|\}$ and

$$\begin{aligned} \max_{\mathcal{G}_{dir}} T_{min}(\mathcal{G}_{dir}) &= \sum_{i=1}^{|\mathcal{N}|-1} i \tau_c \times d(i, i+1) \\ &= \sum_{i=1}^{|\mathcal{N}|-1} i \tau_c \times 1 = \tau_c |\mathcal{N}| (|\mathcal{N}|-1)/2 \leq O(\tau_c |\mathcal{N}|^3). \end{aligned} \quad (46)$$

Otherwise, the worst-case \mathcal{G}_{dir} should have v_l being the first vertex of p that is adjacent to a vertex $\bar{v} \in p$. Then we have

$$\begin{aligned} & \max_{\mathcal{G}_{dir}} T_{min}(\mathcal{G}_{dir}) \\ &= \sum_{i=1}^{l-1} i\tau_c \times d(i, i+1) + \sum_{i=l}^{|\mathcal{N}|-1} i\tau_c \times d(i, i+1) \\ &\leq \sum_{i=1}^{l-1} i\tau_c \times 1 + \sum_{i=l}^{|\mathcal{N}|-1} i\tau_c \times (l-1) \quad (47) \\ &= \frac{1}{2}\tau_c [l(l-1) + (l-1)(|\mathcal{N}|+l-1)(|\mathcal{N}|-l)] \quad (48) \\ &= O(\tau_c |\mathcal{N}|^3), \end{aligned}$$

where eq. (47) holds since no path in \mathcal{G}_{dir} is longer than p , and the maximum of eq. (48) is taken when $l = \lceil \sqrt{3|\mathcal{N}|^2 - 3|\mathcal{N}| + 3}/3 \rceil$. In all, DFS-SG has a $O(\tau_c |\mathcal{N}|^3)$ worst-case communication time. \square

APPENDIX D

GUARANTEES ON APPROXIMATION PERFORMANCE AND DECISION TIME OF DFS-BSG

Theorem 5 (Approximation Performance of DFS-BSG). DFS-BSG enjoys the suboptimality performance,

$$\mathbb{E} [f(\mathcal{A}_t^{\text{DFS-BSG}})] \geq \frac{1}{1 + \kappa_f} f(\mathcal{A}^{\text{OPT}}) - \tilde{O} \left(|\mathcal{N}| \sqrt{|\bar{\mathcal{V}}|/T} \right). \quad (49)$$

Proof: Eq. (49) holds by replacing the bound of EXP3*-SIX in [1, Theorem 2] with that of EXP3 [46]. \square

Theorem 6 (Convergence Time of DFS-BSG). DFS-BSG requires $O[(\tau_f |\bar{\mathcal{V}}| |\mathcal{N}|^2 + \tau_c |\mathcal{N}|^5) |\bar{\mathcal{V}}| / \epsilon]$ time to converge in a directed network, and $O[(\tau_f |\bar{\mathcal{V}}| |\mathcal{N}|^2 + \tau_c |\mathcal{N}|^4) |\bar{\mathcal{V}}| / \epsilon]$ time in an undirected network.

Proof: Since the algorithm requires $O(|\bar{\mathcal{V}}| |\mathcal{N}|^2 / \epsilon)$ rounds to converge per eq. (49), and that in the worst case, each round requires $O(\tau_f |\bar{\mathcal{V}}| + \tau_c |\mathcal{N}|^3)$ time for a directed network and $O(\tau_f |\bar{\mathcal{V}}| + \tau_c |\mathcal{N}|^2)$ time for an undirected network, Theorem 6 holds. \square

APPENDIX E

COMPARISON OF NEISEL WITH NEAREST AND RANDOM NEIGHBOR SELECTION: FROM SPARSE TO DENSE NETWORKS

We also compare ANACONDA with the heuristic benchmarks for neighbor selection (*Nearest Neighbors* and *Random Neighbors*) in 10 scenarios with different network densities. We adjust the network density by deploying the identical 20 cameras to cover areas of 10 different sizes. The results are presented in Fig. 3, where we observe a consistent improvement of ANACONDA across all tested network densities.

Setup. *Environment:* The environment is static and square with areas ranging in $\{200, 400, \dots, 2000\}$. *Agents:* There exist 20 cameras. In each trial, the location x_i of each camera $i \in \mathcal{N}$ is uniformly sampled on the map. They all have the same communication range $c_i = 16$. *Actions:* All cameras

$i \in \mathcal{N}$ have an FOV of radius $r_i = 8$ and AOV $\theta_i = \pi/3$, with direction $a_{i,t}$ chosen from the 16 cardinal directions \mathcal{V}_i , $\forall t$. *Objective Function:* $f(\{a_{i,t}\}_{i \in \mathcal{N}})$ is the total area of interest covered by the cameras \mathcal{N} when they select $\{a_{i,t}\}_{i \in \mathcal{N}}$ as their FOV directions. f is proved to be submodular [3].

Performance Metrics. We evaluate the achieved objective value of the algorithms over 2000 decision rounds.

Results. We observe the improved coordination performance provided by network optimization via NEISEL (Fig. 3). In particular, ANACONDA is comparable or better to the two heuristic benchmarks across all presented network densities. The performance gaps compared to the benchmarks first increase then decrease as the network becomes denser. The reason is that when the network is very sparse, all potential neighbors \mathcal{M}_i are not informative enough to make a difference; when the network is too dense, multiple potential neighbors in \mathcal{M}_i can be informative enough and thus all strategies perform similarly well.